institute of
telecommunications

DIPLOMARBEIT

Receiver Location Sensitivity of Interference Alignment

Ausgeführt zum Zwecke der Erlangung des akademischen Grades eines Diplom-Ingenieurs
unter der Leitung von

Univ.Prof. Dipl.-Ing. Dr.techn. Markus Rupp

und

Dipl.-Ing. Martin Lerch

am

Institute of Telecommunications

eingereicht an der Technischen Universität Wien
Fakultät für Elektrotechnik und Informationstechnik

von

Gerald Artner
0725396
Siebensterngasse 46/3/47a
1070 Wien

Wien, September 2013

Abstract

Modern mobile communication systems are designed based on the cellular principle. The efficiency of such systems is primarily limited by interference from neighboring base stations at the cell edge. In recent years various schemes have been developed to minimize interference through base station cooperation. One such promising scheme is interference alignment (IA). Although theoretically well understood, measurement based evaluations are rare.

Interference alignment (IA) relinquishes half of the available data streams of a mobile connection to align the interference in their subspace and promises an interference free transmission on the remaining data streams. IA uses linear transmit and receive filters and requires global knowledge of the communication channels to calculate these filters. Furthermore IA requires various assumptions regarding the communication channels and the communication network. An important assumption is that the radio channels remain constant from their measurement on to the transmission of the data.

This thesis shows in a scientific, on modern communication systems based, measurement environment that practical channels allow the application of IA and presents measurements that show the impact of changing channels on the efficiency. First the theoretical basics and measurement methods of characteristic figures are summarized. Then the used measurement system, the Vienna MIMO testbed (VMTB), is specified. Differences to a commercial system are clarified and the developed software explained. Additionally the performance of IA under changing channels is quantitatively investigated with the use of mutual information.

Kurzfassung

Moderne mobile Kommunikationssysteme sind nach dem zellulären Prinzip entworfen. Die Effienz solcher Mobilfunksysteme wird primär durch die Interferenz benachbarter Basisstationen am Zellrand limitiert. In den letzten Jahren wurden zahlreiche Schemen erarbeitet, die durch Kooperation der Basisstationen die Interferenz minimieren sollen. Ein vielversprechendes Schema ist Interference Alignment (IA). Obwohl IA theoretisch gut verstanden ist, sind messtechnische Untersuchungen rar.

Interfernce Alignment (IA) verzichtet auf die Hälfte der verfügbaren Datenströme einer Mobilfunkverbindung, um Interferenz in deren Unterraum zu konzentrieren und dann zu verwerfen. In den verbleibenden Datenströmen ist dadurch eine interferenzfreie Übertragung möglich. IA verwendet lineare Sende- und Empfangsfilter und benötigt globale Kenntnis der Kommunikationskanäle zur Berechnung dieser Filter. IA bedarf einiger Annahmen über die Kommunikationskanäle und das Design des Mobilfunknetzes. Eine wichtige Annahme sind konstante Kanäle, da eine erfolgreiche Positionierung der Interferenz nur möglich ist, wenn die Funkkanäle von ihrer Messung bis zur Übertragung der Daten konstant bleiben.

Diese Diplomarbeit zeigt in einer wissenschaftlichen, an modernen Telekommunikationssystemen ausgerichteten Messumgebung, dass in der Praxis auftretende Kanäle den Einsatz von IA erlauben und präsentiert Messergebnisse welche die Auswirkung sich ändernder Kanäle auf die Effizienz darlegen. Zuerst werden die theoretischen Grundlagen und die Messmethoden verwendeter Kennzahlen veranschaulicht. Danach wird der verwendete Messaufbau, das Vienna MIMO testbed (VMTB), spezifiziert. Unterschiede zu einem kommerziellen Telekommunikationssystem werden erläutert und anschließend die im Rahmen dieser Arbeit entwickelte Software vorgestellt. Anschließend wird die Leistung von IA unter veränderlichen Funkkanälen unter Zuhilfenahme der Transinformation (Mutual Information) quantitativ untersucht.

Contents

Chapter 1.

Introduction

A recent trend in modern mobile communication systems it to use smaller cells with more users. In such a setup the interfering signals from other cells limit the overall achievable throughput, especially at the cell edges. Many methods are in use that try to avoid interference by planning mobile communication networks in such a way that users are transmitting in different time slots, different frequencies or are spatially separated.

Recently IA has been proposed to increase channel throughput for the interference channel in the high signal to noise ratio (SNR) regime. IA aligns the interference and the desired signal in different subspaces at the receiver and therefore allows a cancellation of interfering signals. Principles of IA are by now well understood in theory and a few measurements have already been conducted. However the real time feasibility of IA has only been shown in the case of two antennas per node and impairments due to moving receivers have not been investigated.

When new transmission schemes are proposed, the first tests are usually simulations with simplified channel models. Afterwards emulations with measured channels are conducted. Before using new techniques in a commercial system they have to be tested in a laboratory environment. These setups are generally referred to as testbeds. Measurements on testbeds are more expensive and time-consuming than emulations. They yield results that better resemble those obtained at commercial systems than emulations with measured channels and show if a scheme is feasible on available hardware.

The Vienna MIMO testbed (VMTB) is a real time radio frequency system built to evaluate modern multiple input multiple output (MIMO) schemes. This thesis shows the feasibility of IA in a real world MIMO scenario and presents evaluations of the performance of IA with moving receivers.

In Chapter 2 the theoretical channel model, the principle of IA and comparison schemes are introduced. Furthermore characteristic numbers and their estimation in such a system are derived. The VMTB and its current setup are presented in Chapter 3. Differences between this testbed setup and commercial systems are elaborated and the developed software will be explained. In Chapter 4 the acquired measurement results are presented and discussed. Additionally various assumptions needed for the presented evaluation of IA are checked and measurements are provided where necessary. Chapter 5 concludes the results presented in this thesis and discusses their implications on the use of IA in future mobile communication systems.

1.1. State of measurement based Evaluation

To the best of my knowledge the first measurements on IA were presented in [1]. A testbed consisting of 20 universal software radio peripheral (USRP) with two antennas each was used to compare the achieved bit rate to the bit rate of wireless LAN (WLAN) [1].

In [2] IA was emulated with measured channels. A $(2 \times 2, 1)^3$ setup [2] was used to measure static indoor channels, these channels were then used to simulate IA. The paper shows the feasibility of IA in scenarios with real channels, shows how the sum rate changes with varying antenna spacing and provides a measurement of the sum rate for different SNR.

In [3] IA was emulated with channels from a $(2 \times 2, 1)^3$ outdoor and indoor setup. The sum rate of IA is compared to those of time division multiple access (TDMA) and interference avoidance. It is confirmed in [3] that

> [...] IA outperforms TDMA and achieves the maximum degrees of freedom in the three user interference channel and is optimal in the high SNR regime.

[4] presented the first experiments where IA encoded signals were transmitted over physical indoor channels. The $(2 \times 2, 1)^3$ setup used a 4-QAM constellation (binary phase shift keying (BPSK) for the pilots). Typical I-Q-diagram constellations were given for good SNR . The paper also confirmed that IA outperforms TDMA under certain assumptions by comparing their sum rates.

In [5] the same setup as in [4] was used. It shows that the degrees of freedom in such a real time system with imperfect channel state information (CSI) might be lower than the theoretical achievable value.

[6] uses a moveable $(2 \times 2, 1)^3$ indoor testbed. It provides a quantitative comparison between IA and coordinated multi-point (CoMP) and considers imperfect radio equipment.

[7] emulates IA with measured channels in an urban scenario with single antenna nodes. It provides a comparison of various IA algorithms and frequency planning.

[8] analyzes the use of IA for WLAN and provides measured results of bit error rate (BER) and the effects of CSI errors in a typical indoor WLAN setup.

The VMTB is used in [9] to measure the performance of IA under changing SNR and signal to interference ratio (SIR). [9] uses the same testbed setup as described in this thesis.

---

[1]IEEE 802.11

[2]The notation $(M \times N, d)^K$ refers to the MIMO interference channel with K links, each equipped with $M = N$ antennas using d data streams, which is further explained in section 2.1

Chapter 2.

Theory

2.1. Channel Model

A multiple input multiple output (MIMO) channel model consisting of K transmitters with M antennas each and K receivers with N antennas each is considered. Each transmitter transmits d data streams. Let each transmitter $j \in \{1, ..., K\}$ be connected to each receiver $i \in \{1, ..., K\}$ via a complex $M \times N$ channel matrix $\mathbf{H}_{ij} \in \mathbb{C}^{M \times N}$. At each receiver independent white Gaussian noise is added $\mathbf{n}_i \in \mathbb{C}^N$. With a $M \times d$ complex unitary precoding matrix $\mathbf{V}_j \in \mathbb{C}^{M \times d}$ at the transmitter and a $N \times d$ complex unitary interference suppression matrix $\mathbf{U}_j \in \mathbb{C}^{N \times d}$ at the receiver, the received signals $\mathbf{r}_i$ are then connected to the transmit signals $\mathbf{s}_j$ via Equation (2.1).

$$\mathbf{r}_i = \sum_{j=1}^{K} \mathbf{U}_i^H \mathbf{H}_{ij} \mathbf{V}_j \mathbf{s}_j + \mathbf{U}_i^H \mathbf{n}_i \tag{2.1}$$

Figure 2.1 shows a stylized sketch of the proposed channel model. The transmitter with $j = i$ is assumed to be the desired transmitter for receiver i. Transmitters with $j \neq i$ are considered interferers, those channels are depicted by a dashed line in Figure 2.1. Let this model be denoted by $(M \times N, d)^K$.
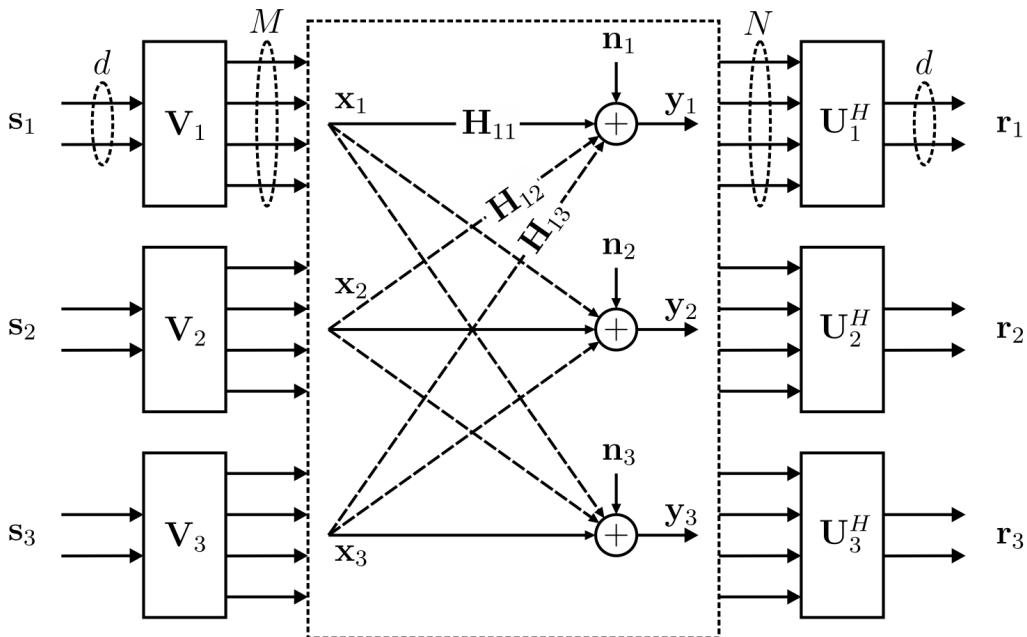

Figure 2.1.: Used MIMO interference channel model

2.2. Channel Model on the Testbed

The $(M \times N, d)^K$ channel model from section 2.1 is updated to fit the specifications of the VMTB. Because three transmitters with four antennas each (supporting four streams) exist in the Vienna MIMO testbed (VMTB), the special case $(4 \times 4, 2)^3$ interference channel model is used in this thesis.

Additionally, due to the cost of a receiver station only one receiver is deployed in the VMTB. This receiver can be logically switched to act as the desired receiver of either transmitter. For example if one wants to measure $\mathbf{y}_1$, then the receiver acts as the desired receiver of transmitter one. To avoid confusion the receiver, that the physical station Rx is used as, will be denoted as the desired link I. This implies that only the channels of the desired link can be measured (depicted as $\mathbf{H}_{1j}$ to the colored receiver in Figure 2.2). The channels from the transmitters to virtual receivers are randomly generated. Each channel from a transmitter to a virtual receiver is a complex 4×4 matrix with independent real and imaginary part that are both normal distributed with zero mean and standard deviation 0.5. Each of these channels is assumed to be independent from the other channels. All transmitters and the receiver, apart from movement on an x-y-ϕ table, are fixed in their places (see Section 3.1). Figure 2.2 shows the updated channel model from section 2.2.
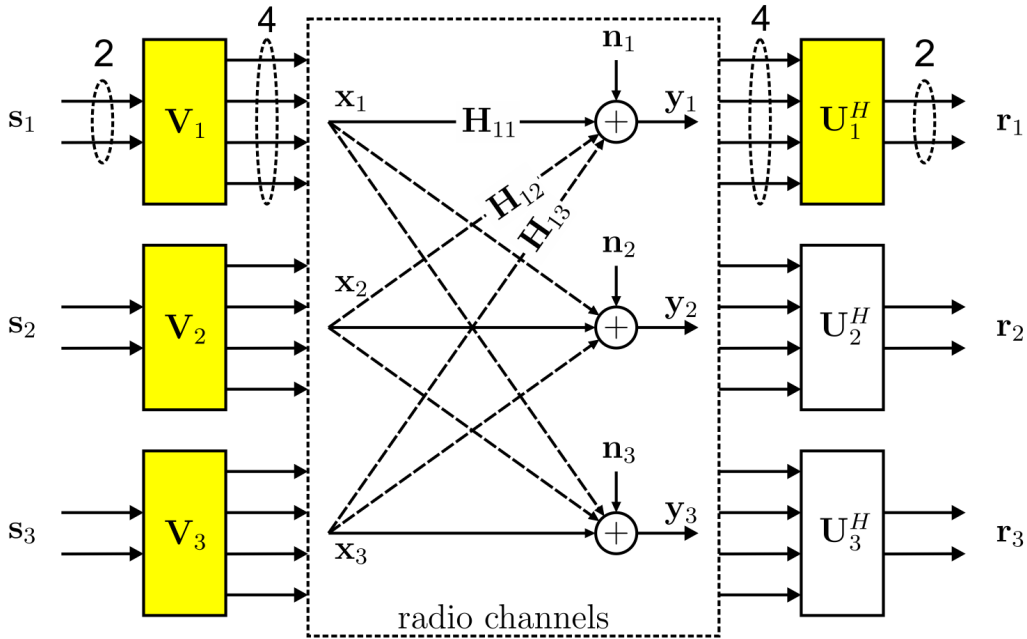

Figure 2.2.: $(4 \times 4, 2)^3$ channel model on the Vienna MIMO testbed. Filled boxes indicate deployed stations. Channels to virtual receivers are random generated. [10]

Channels are expected to change between measurements. Channels estimated during measurement l will be denoted by $\widehat{\mathbf{H}}_{ij}^{(l)}$. Precoding and interference suppression matrices that are calculated from channel estimates of transmission l are denoted as $\mathbf{V}_i^{(l)}$ and $\mathbf{U}_j^{(l)}$. Due to this convention $\widehat{\mathbf{H}}_{ij}^{(l)}$ are used to calculate $\mathbf{V}_i^{(l)}$ and $\mathbf{U}_j^{(l)}$ which are then applied to $\mathbf{H}_{ij}^{(l+1)}$, details can be found in Section 2.4.

Because only one orthogonal frequency-division multiplexing (OFDM) subcarrier is considered in this thesis a notation distinguishing different channels for each subcarrier is not established. Such a notation and the use of IA with more subcarriers are considered in [11].

2.3. Interference Alignment

IA is a linear coding scheme for multi-user interference limited channels. Previously interference was treated as additional noise at the receiver, however it was found that if the interference gets aligned properly this might result in interference free receive signals. It was shown that in a SISO interference model every user can achieve $1/2$ degrees of freedom (DoF) ("half the cake") instead of the previously assumed $1/K$ ("slice of cake") [12]. Various paradigms and techniques to align interference exist, however [13] summarizes that

> Within the class of signal vector space interference alignment schemes, alignment in spatial dimension through multiple antennas (MIMO) is found to be more robust to practical limitations such as frequency offsets than alignment in time or frequency dimensions.

In this thesis spatial IA is considered. IA requires high SNR, global knowledge of the channels and a transmit filter as well as a receive filter. The transmit filters $\mathbf{V}$ align the interfering signals in the nullspace of the desired signals at each receiver. The receive filters $\mathbf{U}$ are then used to project the whole signal to an interference free subspace.

In the channel model from section 2.1 the jth transmitter is considered the desired transmitter for receiver i if $j = i$. The transmitters $j \neq i$ are considered interferers. Equation (2.1) can then be split up into desired signal, interfering signal and noise.

$$\mathbf{r}_i = \underbrace{\mathbf{U}_i^H \mathbf{H}_{ii} \mathbf{V}_i \mathbf{s}_i}_{\text{desired signal for receiver i}} + \underbrace{\sum_{j \neq i} \mathbf{U}_i^H \mathbf{H}_{ij} \mathbf{V}_j \mathbf{s}_j}_{\text{interfering signal for receiver i}} + \underbrace{\mathbf{U}_i^H \mathbf{n}_i}_{\text{effective noise}} \tag{2.2}$$

According to [14] the goal of IA is to find $\mathbf{U}$ and $\mathbf{V}$ such that the interference is zero at the receivers

$$\mathbf{U}_i^{\mathbf{H}} \mathbf{H}_{ij} \mathbf{V}_j = 0, \ \forall j \neq i \tag{2.3}$$

and the resulting channels have full rank

$$\text{rank}(\mathbf{U}_i^H \mathbf{H}_{ii} \mathbf{V}_i) = d, \ \forall i \in \{1, ..., K\} \tag{2.4}$$

In that case the channel model from section 2.1 can be simplified to a $d \times d$ MIMO channel with channel coefficients $\mathbf{U}_i^H \mathbf{H}_{ii} \mathbf{V}_i$ for each receiver i. A necessary condition for symmetric systems was presented in [13, theorem 1] and can be found in Equation (2.5).

$$M + N \geq d(K + 1) \tag{2.5}$$

Equation (2.5) limits the number of streams for a given number of antennas at receiver and transmitter. In practical systems this condition might be sufficient for IA to work.

The channel matrices $\mathbf{H}_{ij}$ are needed to compute $\mathbf{U}$ and $\mathbf{V}$. In a practical system the estimated channel matrices denoted as $\widehat{\mathbf{H}}_{ij}$ are used. Channel estimation with a least squares (LS) approach on the VMTB is discussed in section 2.4.3. Various algorithms for the IA problem have been proposed. An iterative algorithm for calculating $\mathbf{U}$ and $\mathbf{V}$ from the channel matrices has been proposed in [14]. For up to three receiver-transmitter pairs $K \leq 3$ an analytical solution exists [12]. In this thesis IA is implemented using the analytical solution, because it was found to be much faster than most algorithms.

2.4. Implementation

This chapter presents the implementation of IA on the VMTB. It is shown how the changing channels are considered and how characteristic numbers are estimated. Furthermore the functionality of the developed software is discussed. Each data packet is prefixed by channel estimation pilots. The channel estimates $\widehat{\mathbf{H}}_{ij}^{(l)}$ are used to calculate the IA matrices. Because the calculation of $\widehat{\mathbf{H}}_{ij}^{(l)}$ from the pilots and the generation of the transmit signals takes some time T_p, it is expected that the channel changes until the precoded signal is transmitted. The channel estimates acquired from these pilots are also a measure of how much the channel changes between transmissions. $\widehat{\mathbf{H}}_{ij}^{(l+1)}$ is therefore a measure of the channel at the time the signal encoded with $\mathbf{V}_i^{(l)}$ was actually transmitted. The relationship between channel estimates and precoders in consecutive transmission frames is depicted in Figure 2.3.
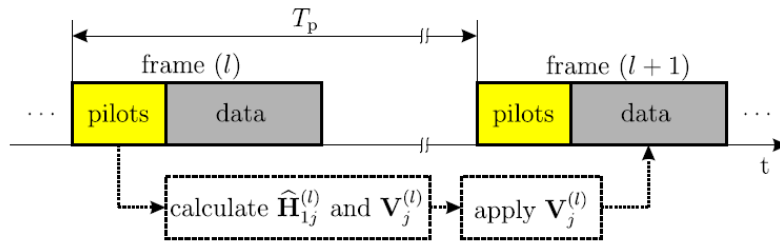

Figure 2.3.: Relationship between channel estimates, precoders and frames [10]

In order to measure the mutual information presented in Section 2.4.2 the transmitted data is split up into two stages. During the first stage both the desired transmitter and the interferers transmit data, during the second stage only the interferers transmit. Noise is present during both stages.
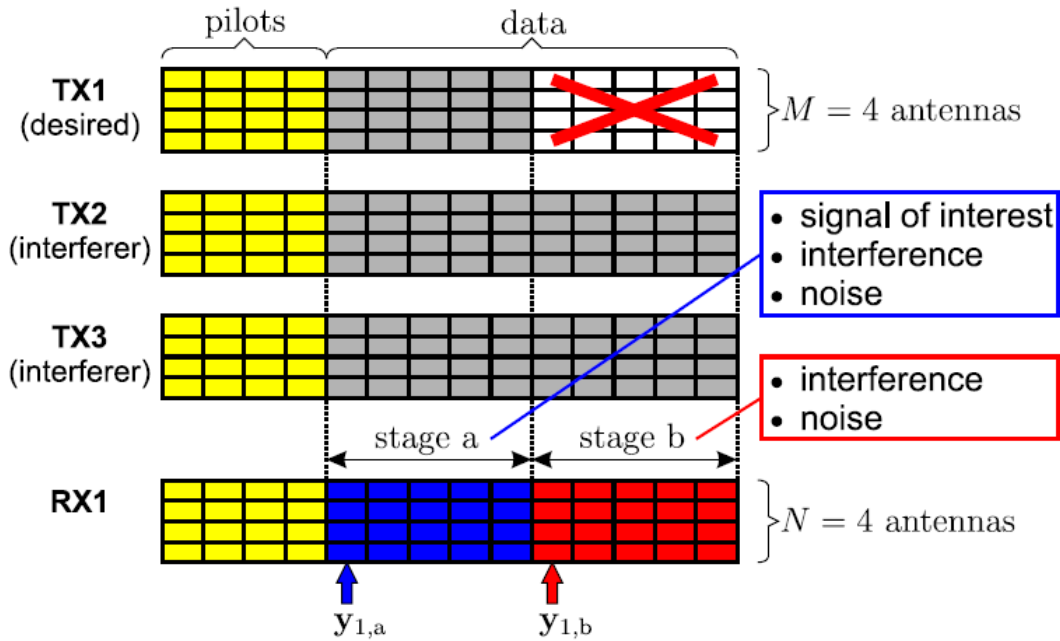

Figure 2.4.: Transmit and receive signal design to measure mutual information [10]

Figure 2.4 shows how the data is split up in the transmit signals in order to measure mutual information on the receiver. This approach allows a measurement of the mutual information of the desired link as

$$\mathcal{I}_{\widehat{\mathbf{Q}}}(\mathbf{s}_I; \mathbf{y}_I) = \log_2 \det\left(\widehat{\mathbf{Q}}_{\mathrm{a}} \widehat{\mathbf{Q}}_{\mathrm{b}}^{-1}\right) \tag{2.6}$$

with the covariance matrices of the respective stages

$$\widehat{\mathbf{Q}}_{\mathrm{a}} = \mathrm{E}\{\mathbf{y}_{1,\mathrm{a}} \mathbf{y}_{1,\mathrm{a}}^H\} \tag{2.7}$$

$$\widehat{\mathbf{Q}}_{\mathrm{b}} = \mathrm{E}\{\mathbf{y}_{1,\mathrm{b}} \mathbf{y}_{1,\mathrm{b}}^H\} \tag{2.8}$$

where a and b refer to different stages of data as depicted in Figure 2.4. The derivation of Equations (2.6) to (2.8) can be found in [10].

2.4.1. Singular Value Decomposition

As a comparison to IA a scheme with filters, that are a solution of the singular value decomposition (SVD) of the channel, was chosen [15]. This scheme is also referred to as dominant eigenmode transmission. The SVD can be used both as an upper and lower bound for the performance of IA.
The SVD of the channel matrix $\mathbf{H}_{Ij}$ from transmitter j to its desired receiver I is defined as

$$\mathbf{H}_{Ij} = \mathbf{L}_I \mathbf{\Sigma}_{Ij} \mathbf{R}_j^H \tag{2.9}$$

The upper bound is achieved if no interferers are present. In this case IA sacrifices half of the available streams to align the interference in this subspace. This is suboptimal because no interference is present and only half the streams can be utilized. In such cases SVD performs better because it keeps all streams.
The lower bound is found if interferers are present. IA then uses half of the streams to align the interference at each receiver in these subspaces. Because each transmitter calculates the SVD using the channel to the desired transmitter and ignores the interferers, the desired signals and the interfering signals overlap at the receivers. In this case IA performs better because instead of "shouting down" each other, every receiver gets "half the cake".
For IA global knowledge of the channels between all transmitters and receivers is required while only the knowledge of the desired link is needed to calculate the SVD. If the channel changes too much it won't be possible to align the interference at the receivers properly and it is expected that SVD outperforms IA. In this work this will be particularly important because a moving receiver causes channel changes. When designing a communication system that utilizes IA this leads to a tradeoff between the frequency at which channels are estimated and the speed of the receivers.

2.4.2. Mutual Information

The mutual information (MI) is a measure for the dependence of two random variables. In this work MI is used to quantify the amount of data that can be transferred from the transmitters to the desired receivers. The used methods to estimate the MI are presented.

The MI between the signal a and b is denoted by $\mathcal{I}(a;b)$. Two different sources are used in this thesis to estimate the mutual information, the estimated channels and the covariance matrices of the received signal symbols. MI estimated from the covariance matrices of the received symbols is based on signals transmitted over the VMTB with applied IA precoders. To indicate the underlying source of the MI, MI calculated from estimated channels is denoted by $\mathcal{I}_{\widehat{\mathbf{H}}}(a;b)$ and MI calculated from the covariance matrices of the received symbols is denoted by $\mathcal{I}_{\widehat{\mathbf{Q}}}(a;b)$. The achievable MI without interferers is indicated by $\mathcal{I}_{\mathrm{noInt}}(a;b)$. SVD is used as a comparison to IA. If the MI is calculated for filters resulting from the SVD instead of the IA filters this is indicated by $\mathcal{I}_{\mathrm{SVD}}(a;b)$. The used signals can be found in Figure 2.4. To measure the effect of outdated CSI, the IA solution of the first transmission is kept for the whole measurement. If MI is calculated with the filters of the first transmission, this is denoted by $\mathcal{I}^{(1)}(a;b)$.

The MI derived from the received symbols is calculated as

$$\mathcal{I}_{\widehat{\mathbf{Q}}}(\mathbf{s}_I;\mathbf{y}_I) = \log_2 \det\left(\widehat{\mathbf{Q}}_{\mathrm{a}}\widehat{\mathbf{Q}}_{\mathrm{b}}^{-1}\right) \tag{2.10}$$

Equation (2.10) is derived in [10, Eq. 10].

MI between the transmit and receive streams is calculated as

$$\mathcal{I}_{\widehat{\mathbf{H}}}(\mathbf{s}_I;\mathbf{r}_I) =$$

$$\log_2 \det\left(\mathbf{I} + \mathbf{U}_I^H\widehat{\mathbf{H}}_{II}\mathbf{V}_I\left(\mathbf{U}_I^H\widehat{\mathbf{H}}_{II}\mathbf{V}_I\right)^H \left(\sum_{j\neq I}^{K}\mathbf{U}_I^H\widehat{\mathbf{H}}_{Ij}\mathbf{V}_j\left(\mathbf{U}_I^H\widehat{\mathbf{H}}_{Ij}\mathbf{V}_j\right)^H + \mathbf{U}_I^H\widehat{\mathbf{Q}}_N\mathbf{U}_I\right)^{-1}\right),$$
$$\tag{2.11}$$

MI from the channel estimates without applied receive filters $\mathbf{U}_I$ is calculated between $\mathbf{s}_I$ and $\mathbf{y}_I$ as

$$\mathcal{I}_{\widehat{\mathbf{H}}}(\mathbf{s}_I;\mathbf{y}_I) = \log_2 \det\left(\mathbf{I} + \widehat{\mathbf{H}}_{II}\mathbf{V}_I\left(\widehat{\mathbf{H}}_{II}\mathbf{V}_I\right)^H \left(\sum_{j\neq I}^{K}\widehat{\mathbf{H}}_{Ij}\mathbf{V}_j\left(\widehat{\mathbf{H}}_{Ij}\mathbf{V}_j\right)^H + \widehat{\mathbf{Q}}_N\right)^{-1}\right). \tag{2.12}$$

The MI of the desired link is calculated between the signals $\mathbf{x}_I$ and $\mathbf{y}_I$ as

$$\mathcal{I}_{\widehat{\mathbf{H}}}(\mathbf{x}_I;\mathbf{y}_I) = \log_2 \det\left(\mathbf{I} + \widehat{\mathbf{H}}_{II}\widehat{\mathbf{H}}_{II}^H \left(\sum_{j\neq I}^{K}\widehat{\mathbf{H}}_{Ij}\widehat{\mathbf{H}}_{Ij}^H + \widehat{\mathbf{Q}}_N\right)^{-1}\right) \tag{2.13}$$

When calculating $\mathcal{I}_{\widehat{\mathbf{H}},\mathrm{SVD}}$ the matrices $\mathbf{U}$ and $\mathbf{V}$ in Equations (2.11) to (2.13) are replaced with the matrices $\mathbf{L}$ and $\mathbf{R}$ from the SVD solution.

To calculate the MI with the filters of the first transmission $\mathcal{I}_{\widehat{\mathbf{H}}}^{(1)}$, $\widehat{\mathbf{H}}^{(l)}$ is taken from the l-th transmission while $\mathbf{U}^{(1)}$ and $\mathbf{V}^{(1)}$ from the first transmission are used in Equations (2.11) to (2.13).

To calculate the MI without interferers $\mathcal{I}_{\widehat{\mathbf{H}},\mathrm{noInt}}$, the sums in Equations (2.11) to (2.13) are set to zero.

When the desired transmitter is turned off, the MI becomes zero. However, due to numerical and estimation errors the measured MI might only be close to zero. Such cases will be denoted by $\mathcal{I}_{\widehat{\mathbf{Q}},\mathrm{noDes}}$.

2.4.3. Channel Estimation

IA requires knowledge of the radio frequency channels between the transmitters and receivers. These channels are often estimated by transmitting a sequence of known symbols called pilots. The receiver compares the received symbols to the known sent symbols to estimate the channel. There exist various methods for pilot based channel estimation. A least squares (LS) approach was chosen for channel estimation. Because the channel from each transmit antenna has to be estimated, there have to be at least $M \cdot K = 4 \cdot 3 = 12$ pilot symbols. The pilot sequences presented in [16] are based on Zadoff-Chu sequences and are optimized for LS channel estimation. They are orthogonal to shifted versions of themselves which makes them easy to generate. Each transmitter transmits a cyclic time-shifted version of the pilot sequence at each antenna and the receiver calculates the correlation of the received signal with this shifted sequence to get the channel to the corresponding transmitter and antenna.

Note that such an estimated channel does not only include the air interface, but the whole OFDM chain between the transmitted and received signal and thus incorporates the characteristics of radio equipment.

The following sequence was chosen from [16, Appendix A]

$$S^P = (1,\ 1,\ 1,\ 1,\ 1,\ j,\ -1,\ -j,\ 1,\ -1,\ 1,\ -1,\ 1,\ -j,\ -1,\ j) \tag{2.14}$$

2.4.4. Distribution of CSI

In a mobile communication system the distribution of channel state information (CSI) becomes a challenge. The channel estimates have to be collected from the receivers and distributed to all nodes in order to compute $\mathbf{U}$ and $\mathbf{V}$, equivalently the CSI can be collected at one node and $\mathbf{U}$ and $\mathbf{V}$ distributed. Regardless of the approach the challenge to distribute matrices among all nodes remains. At the current state of the art the main problems are:

- the elements of the matrices have to be transmitted with finite precision and therefore be quantized

- because the channel estimates will be feed back over the air interface they can be expected to be received erroneous

- the feedback of CSI introduces an additional delay

- in case the channel estimates are fed back over a different channel (e.g. on a different frequency) than this channel might have to be estimated as well

Because these issues are still ongoing research at the time of writing, they were avoided on the current installation of the VMTB. The nodes of the VMTB are connected through a glass fiber network that is used to synchronize the nodes and to send transmit symbols to the transmitter stations. In this work the fiber network is used to transmit the precoding matrices $\mathbf{V}$ to the transmitters at floating point precision. This is a typical approach in testbed aided evaluation of IA.

Another reason not to distribute the CSI over the air interface on the VMTB is that Rx is not capable of transmitting data and the transmit stations not capable of receiving.

Chapter 3.

System Characterization

3.1. Vienna MIMO Testbed

The Vienna MIMO testbed (VMTB) is a rapid prototyping MIMO system for radio frequency measurements. It consists of three transmitters and a receiver that are fixated on wooden desks on wheels [17, pg. 2] [18, pg. 2]. This way hardware can be moved easily which allows an adaption of the testbed to measure different scenarios. Measurements can be fully conducted in Matlab. In this chapter the current specifications and setup of the VMTB as well as an overview about its functionality and references to more detailed descriptions are given. Note that the VMTB is constantly upgraded. Changes made to the testbed since the cited publications are illustrated in newer publications or in this thesis.

The VMTB has recently been used to evaluate different antenna configurations in the LTE MIMO downlink [19].

Descriptions of older versions of the VMTB can be found in [20] and [21].

The positions of the nodes are shown in Figure 3.1. The antennas of Tx1 are located on the roof of the TU building at Favoritenstraße 9-11, the transmitter station depicted in Figure 3.2 is located in a storage room on the roof. The antennas of Tx2 are on the roof of the TU building "neues EI" at Gußhausstraße 27-29, the transmitter station is in the library of the automation and control institute. Tx3 an Rx are located indoor on the fifth floor of the "altes EI" building at Gußhausstraße 25 in the institute of telecommunications.
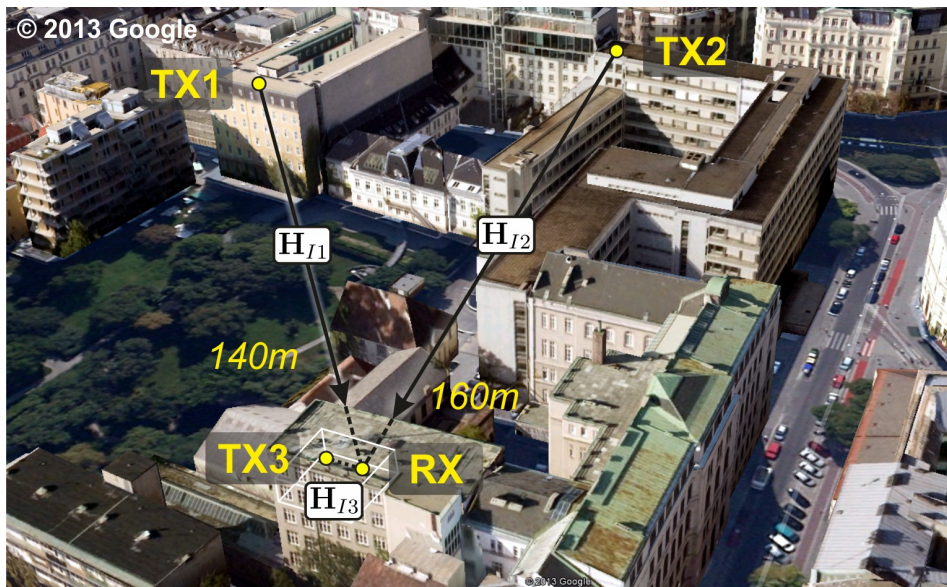
Additional information about the VMTB an be found in [17].

Figure 3.1.: Location of nodes, location of Tx3 has changed from that used in [10]

3.1.1. Specifications

The transmitter hardware, software, available commands and measurements of hardware characteristics are described in [18]. The receiver is described in [22]. A photo of transmitter station Tx1 can be seen in Figure 3.2. The stations at Tx1, Tx2 and Tx3 are identical.
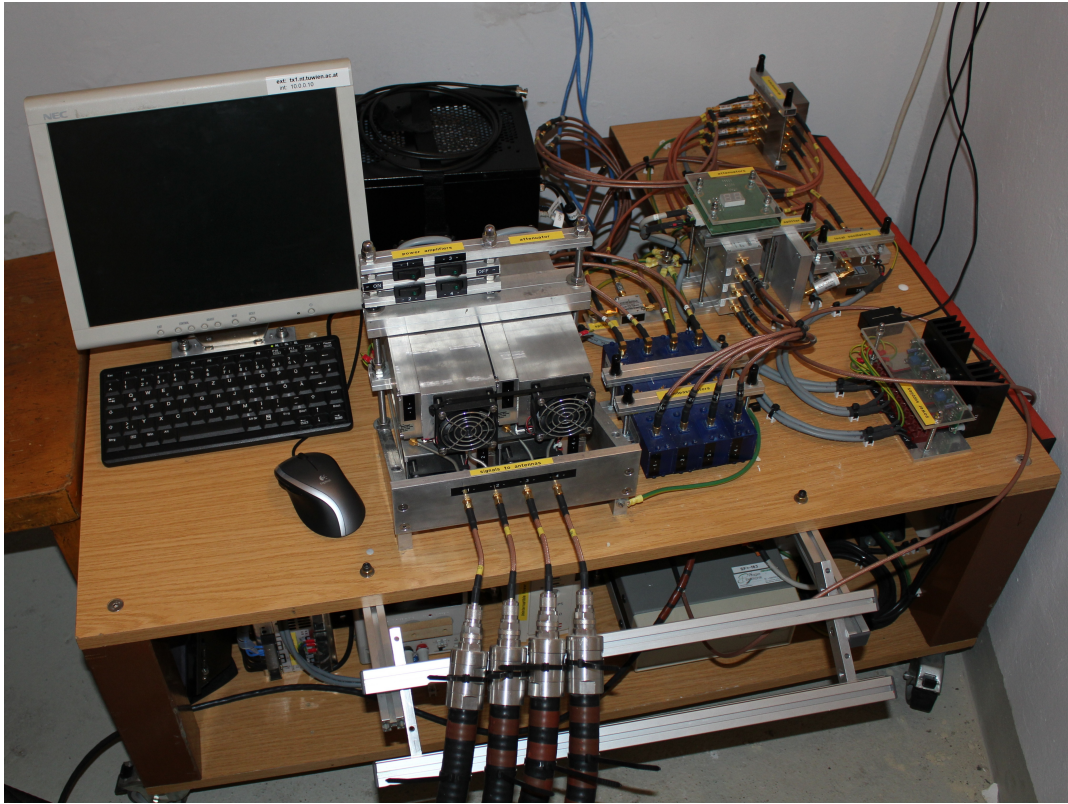

Figure 3.2.: Transmitter station Tx1.

The personal computer (PC)

> contains an Intel Core i7 central processing unit (CPU), 6GB of dynamic random access memory (DRAM), a flash storage and an Innovative X5-TX module for the digital to analog conversion of the offline generated transmit data. [18, pg. 3]

A block diagram of the transmitter chain can be seen in Figure 3.3.

The hardware used in the transmitter stations according to [18, pg. 4] consists of: The MITEQ DLCRO local oscillator operates at 2.433 GHz. The filter is a surface acoustic wave (SAW) filter with 20 MHz bandwidth. The digitally programmable attenuator is an AEROFLEX 4226 and ranges from 0 to 63 dB. The power amplifier is a KU PA 2426 A has a nominal gain of roughly 55 dB.

Tx1 and Tx2 each use a Kathrein 800 10543 XXpol antenna[23]. Tx3 uses two Kathrein 800 10677 Xpol indoor antennas[24].

The fixation of the Tx1 antenna is depicted in fig. 3.4 and the fixation of the Tx2 antenna in Figure 3.5.

The receiver node is depicted in Figure 3.6. The receiver station is on the left side. On the right side is a laptop chassis mounted on an x-y-ϕ table. The four antennas are inside the laptop chassis and resemble a future WLAN or UMTS long term evolution (LTE) equipment.
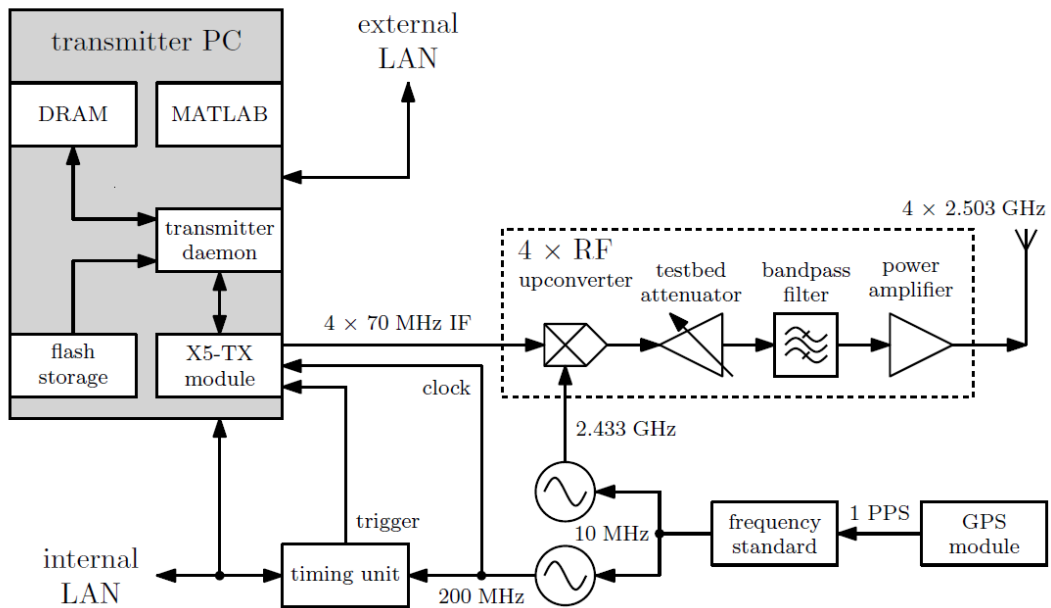
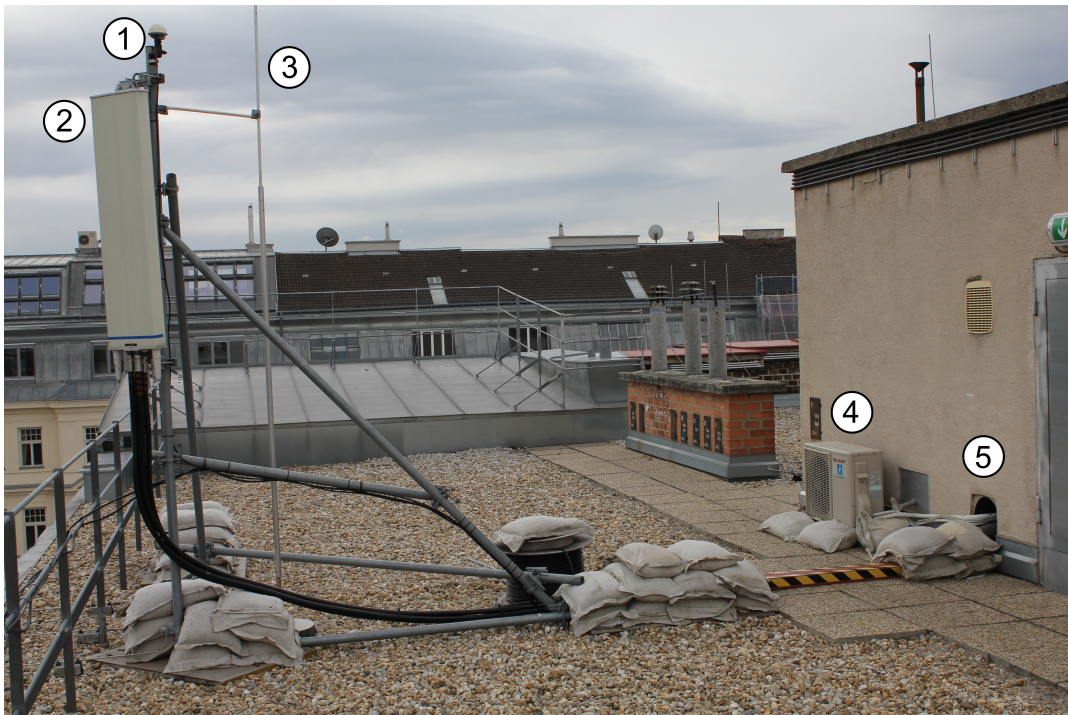**Figure 3.3.:** Blockdiagram of the transmitter chain [18, pg. 2, figure 2.1]

Figure 3.4.: Antenna setup of Tx1: 1 GPS, 2 antenna, 3 lightning arrester, 4 air conditioner, 5 connection to transmitter station
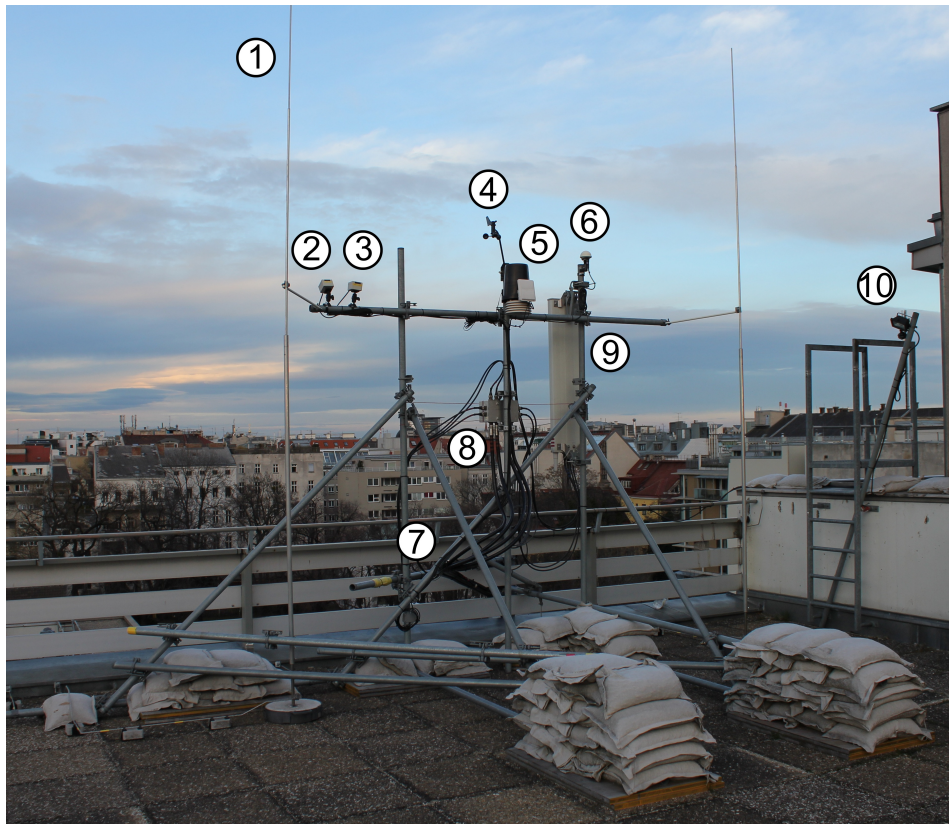
Figure 3.5.: Antenna setup of Tx2: 1 lightning arrester, 2 rain sensor, 3 fog sensor, 4 wind speed sensor, 5 precipitation amount sensor, 6 GPS, 7 webcam (not visible) , 8 antenna switch, 9 antenna, 10 lamp
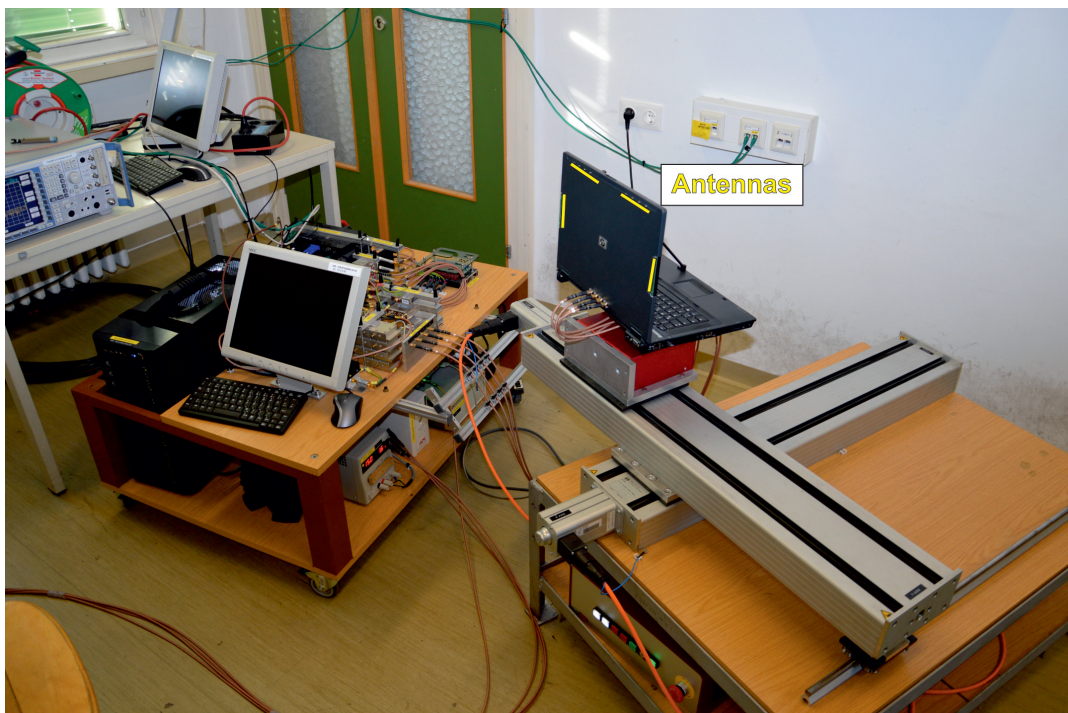

Figure 3.6.: Receiver setup of Rx: receiver station (left) and antennas on x-y-ϕ table (right)

The hardware used in the receiver station: The analog to digital converter (ADC) is a X5-RX PCI Express card from Innovative Integration. The preamplifier is a ZFL-500HLN from Mini-Circuits. The PC has an Intel i7 CPU with 3.2 GHz, it was upgraded to 24 GB of DRAM and runs Windows 7 Enterprise. Four $\lambda/2$ dipole antennas are included into the laptop chassis.

A block diagram of the receiver chain can be found in fig. 3.7 and a block diagram of the receivers radio front end in fig. 3.8.
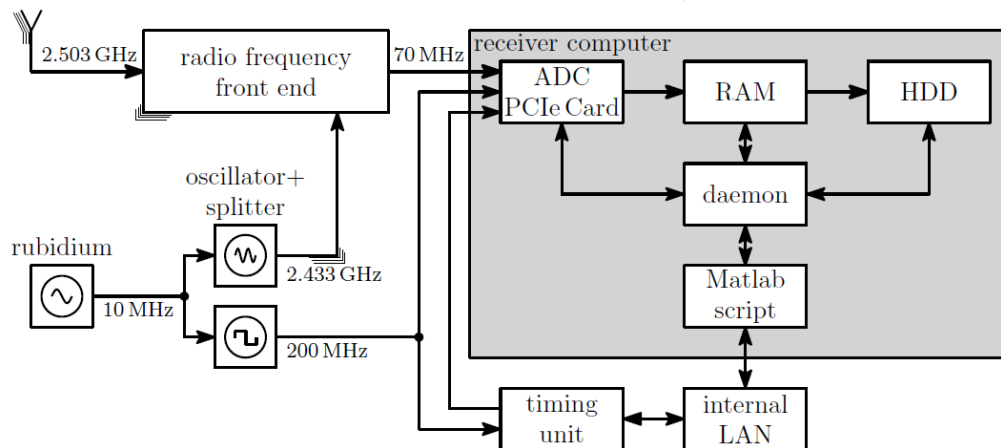
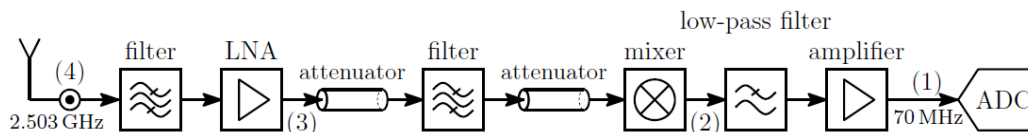**Figure 3.7.:** Block diagram of receiver chain [22, pg. 2, figure 1.1]

Figure 3.8.: Radio front end at the receiver [22, pg. 34, figure 3.5]

3.1.2. Synchronization

Synchronization is a common problem in mobile communications as participating nodes often lack a common reference clock. In order to suppress effects of poor synchronization on the measurement results, the VMTB runs a subsystem that keeps the nodes synchronized. An investigation of this subsystem, its timing unit and the synchronization of the VMTB can be found in [25]. Each node is connected to a Trimble Acutime global positioning system (GPS) receiver, a Stanford Research Systems rubidium FS725 reference frequency standard, a timing unit and a dedicated fiber local area network (LAN). Those are used to keep the nodes synchronized.

The signals from the different transmitters are received at Rx with different delays. Because of the synchronization between the nodes these delays can be seen as constant. Therefore, these delays can be compensated by a constant shift of the transmitter samples and are received simultaneously at the receiver.

3.2. Comparison to commercial mobile Communication Systems

Testbeds are often used to investigate if theoretical schemes with simplified models could be applied in a (future) commercial system. However, to resemble a wider range of possbile implementations, to perform scientific measurements, economic reasons and because of an uncertainty regarding future standards, testbeds differ from commercial setups. Although all specifications of the testbed and schemes are presented throughout this thesis it is nice to have a comparison between the measurement setup used in this thesis and (possible) commercial realizations of mobile communication systems. This chapter does not compare the used measurement setup to theoretical models because the used model is simple and was already presented in sections 2.1 and 2.2.

- **Channel Estimation** can be expected to yield results closer to the "real" channel, because the pilot sequence is transmitted in adjacent time symbols on a single subcarrier. In a commercial system pilot symbols will be distributed over time and frequency and will be interpolated. Note that the testbed approach is not practical as it results in significant overhead for channel estimation.

- **Distribution of CSI** is an enormous problem in practical communication system as it introduces delays and errors to the CSI and lowers the throughput. Because the exact execution of CSI distribution is still ongoing research it was idealized by a dedicated glass fiber link on the testbed, resulting in low delays and allowing CSI with floating point precision.

- **Calculations** on the testbed are mostly performed in Matlab. Compared to hardware implementations in commercial system they take a tremendous amount of time. Received signals have to be stored for offline evaluation, which introduces significant delays on the testbed.

- **Synchronization** on the VMTB is really good because of the used Rubidium frequency normals. This is a common design choice in measurement systems if the effects of bad synchronization are not of interest. It can be expected that mobile devices are not as good synchronized in frequency and time.

- **Transmitter Antenna Setup** and positioning as presented in section 3.1 are equivalent to current base stations.

- **Receive Antenna Setup** is a realistic setup for a laptop.

- **Scenario**: The current setup of the VMTB presents a realistic scenario with an indoor mobile station. The intention behind the setup is to have two outdoor base stations and an indoor transmitter accounting for the future use of micro- or femto cells. It can however also be interpreted as a WLAN router with interfering routers outside the room.

- **The Frequency Band** are commercial frequencies provided by A1 Telekom Austria and, unlike other testbeds that operate in the industrial, scientific and medical (ISM) band, interference from the outside doesn't occur.

- **Laboratory grade RF Equipment** is used for the filters, amplifiers, cables etc. on the testbed.

3.3. Software

Most of the software is written in Matlab and runs on Rx. This software generates the transmit symbols. It reads the received samples from the ADC card, estimates the channels from them and stores them for offline evaluation. It calculates the IA solution and distributes the precoding matrices to the transmitters. It controls the flow of a measurement and moves the x-y-ϕ table. Additionally it manages the settings and provides a user interface.

Programs for offline evaluation, merging and presentation of the evaluated data are also written in Matlab but can be run on any computer.

The transmitters run C++ programs that calculate the transmit samples and write them to the digital to analog converter (DAC) cards.

A program that remote controls switches and collects data from the weather stations exists. Computers have wake on LAN functionality and can be woken by a Matlab script. Almost all hardware is monitored by webcams that can be accessed via their web interfaces.

3.3.1. Transmitter implementation

C++ programs, which are updated versions of the transmitter daemon presented in [18], run on Tx1, Tx2 and Tx3. These programs calculate the transmit signals in real time. In addition to the available functions the daemons were updated to perform the IA precoding of the data and allow different transmit powers for data and pilots.

The updated reset command from [18, pg. 23, ff.] has an additional set of parameters ia_params. ia_params consists of 4 parameters: startIndex, numSymbols, numSamplesPer-Symbol and DACScaling. They are separated by a semicolon. Table 3.1 shows the new structure of the transmitter reset command, the new parameters for interference alignment are shown in Table 3.2. *DACScaling* in Table 3.2 is used to get the full possible DAC range of 16 bit. To control the output power of the transmitters the *Sync_IO* parameters in the HIATUS (Table 3.3) command should be used as they control the transmitters attenuators. In the Matlab implementation on Rx they can be easily accessed via the variable *testbedAttenuators* in the settings.

command	**RST** |*file_name* |*channels* |*block_size* |*block_split_factor* |*load_split_factor* |*loading_timeout* |*sending_timeout* |*trigger_delay* |*transmit_mode* |*verbose_mode* |***ia_params***
new parameters	**string** *ia_params* contains the additional parameters needed for this project

Table 3.1.: The updated transmitter reset command

startIndex	**int32**	%d	index where the data samples start
numSymbols	**int32**	%d	number of transmit symbols
numSamplesPerSymbol	**int32**	%d	number of passband samples per symbol
DACScaling	**double**	%e	scaling of the Tx DAC Card

Table 3.2.: The parameters set in ia_params in the RST command

The updated version of the transmit command [18, pg. 25, ff.] is shown in Table 3.3. The command was renamed to HIATUS, the block offset factors were removed and an additional parameter set *ia_ params* was added. The parameters in *ia_ params* are separated by semicolon.

command	**HIATUS** |*Sync_ IO_ 1* |*Sync_ IO_ 2* |*Sync_ IO_ 3* |*DAC1_ gain* |*DAC2_ gain* |*DAC3_ gain* |*DAC4_ gain* |*repetition* |*trigger_ repetition* |***ia_ params***
new parameters	**string** *ia_ params* contains the additional parameters needed for this project

Table 3.3.: The updated transmitter transmit command

TxSymbols	**int8**	%d	transmit data symbols
Vre	**double**	%f	real part of **V**
Vim	**double**	%f	imaginary part of **V**

Table 3.4.: The parameters set in ia_params in the HIATUS command

The pilot samples are stored in a file that gets loaded with the reset command and are then automatically prefixed to every transmission with the HIATUS command. The file is referenced with *file_ name* in the RST command, they are the same in each transmission. The parameters in *ia_ params* are separated by semicolon, the symbols are separated by comma. *TxSymbols* contains the first stream of transmit symbols first, the second stream is appended.

Because only five different transmit symbols are needed for 4-QAM, they are encoded in int8 for *TxSymbols* according to Table 3.5. The real and imaginary parts of **V** are sorted for *Vre* and *Vim* as: V(1,1), V(2,1), V(3,1), V(4,1), V(1,2),...

Symbol in IQ-diagram	encoded for HIATUS command
0	0
$1 + j$	1
$-1 + j$	2
$-1 - j$	3
$1 - j$	4

Table 3.5.: Encoding of the data symbols for the HIATUS command

3.3.2. Receiver

Most of the calculations are performed on Rx and the receiver handles the flow of the measurements and possible errors. The Matlab program on Rx reads the received samples from the RAMdisk, estimates the channels, calculates the IA matrices $\mathbf{U}$ and $\mathbf{V}$, sends the precoding matrices to the transmitters, moves the x-y-ϕ table and stores the channel matrices and received signals for offline evaluation.

The initialization of a measurement can be seen in Figure 3.9, Figure 3.10 shows the program flow while transmitting. All settings are stored in loadSettings.m and are checked for plausibility with various tests defined in checkSettings.m. Some matrices and vectors are calculated before transmissions start to reduce the time between transmissions, a few examples are: Upmix multipliers, indices where pilots and data start in vectors, pilot samples and data symbols. During testbed startup various parameters such as block length, buffer size or packet length are set. Testbed checks include pinging the daemons, checking if GPS is running, the rubidium clock is running, checking address resolution protocol (ARP) tables and calibration of the DACs. Connecting with the demons include transmission of symbol and DAC scaling and sending reset signals to the daemons.

Because the used transmission scheme is a standard OFDM chain, it is not depicted here. Detailed descriptions of OFDM systems with IA can be found in [9] [11].

3.3.3. Offline Evaluation

In order to speed up the measurement, characteristic numbers that are used to evaluate the performance of IA and are not necessary for IA to work are calculated offline after the measurements are finished. This is a typical simplification to speed up the measurement process that was used on other testbeds, it doesn't influence the performance comparison because not all of these numbers are used for scientific evaluation and will not be calculated in a commercial system. The following numbers are calculated offline with the evaluation program: Mutual information, eigenvalue separation of the received interference only data, decoded received symbols, symbol error rate, symbol errors per transmission, mean squared error (MSE) from the received symbols to their desired position in the I-Q-diagram, average MSE per transmission, noise power, received power from each transmitter, SNR and various metrics for channel change.
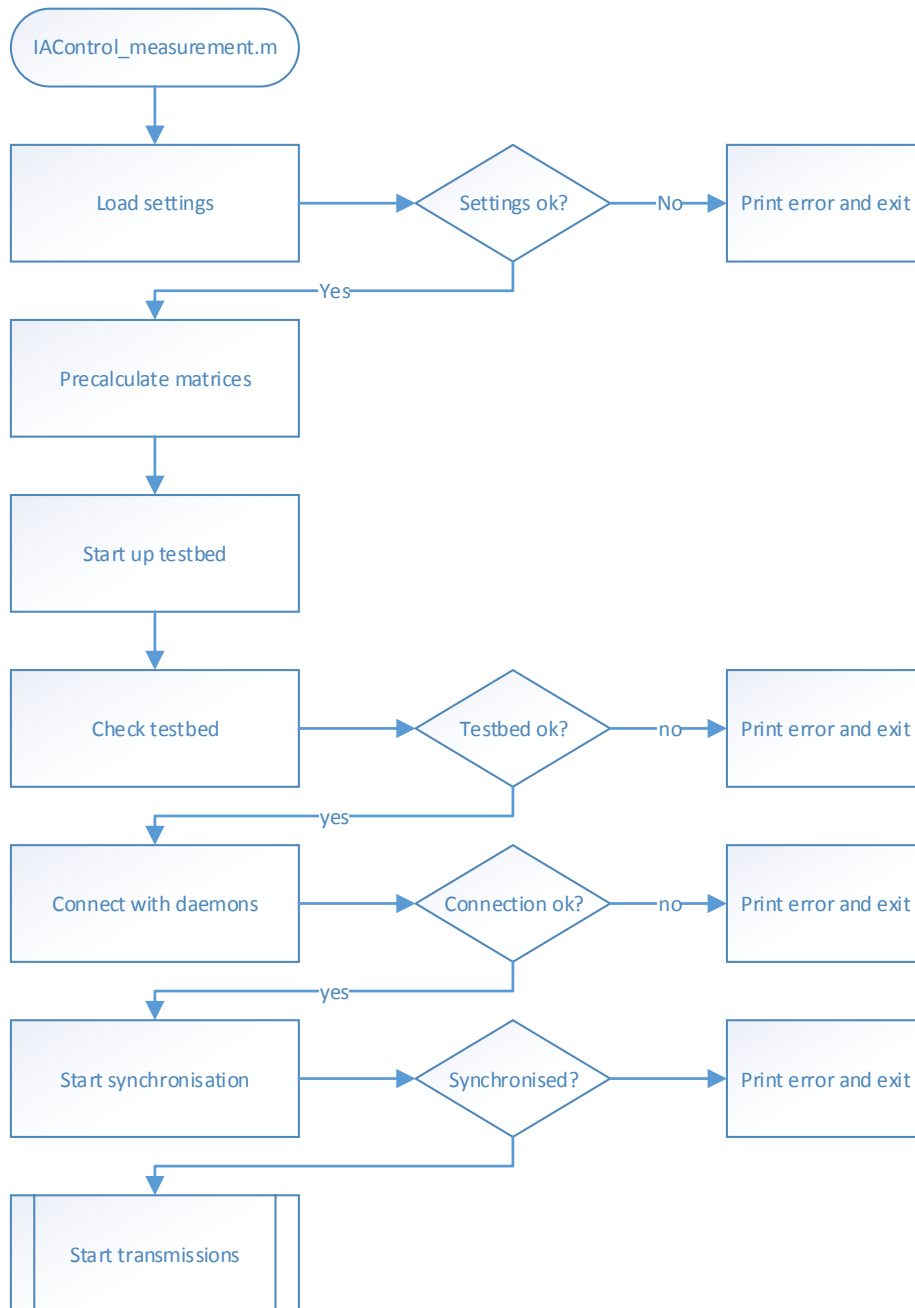
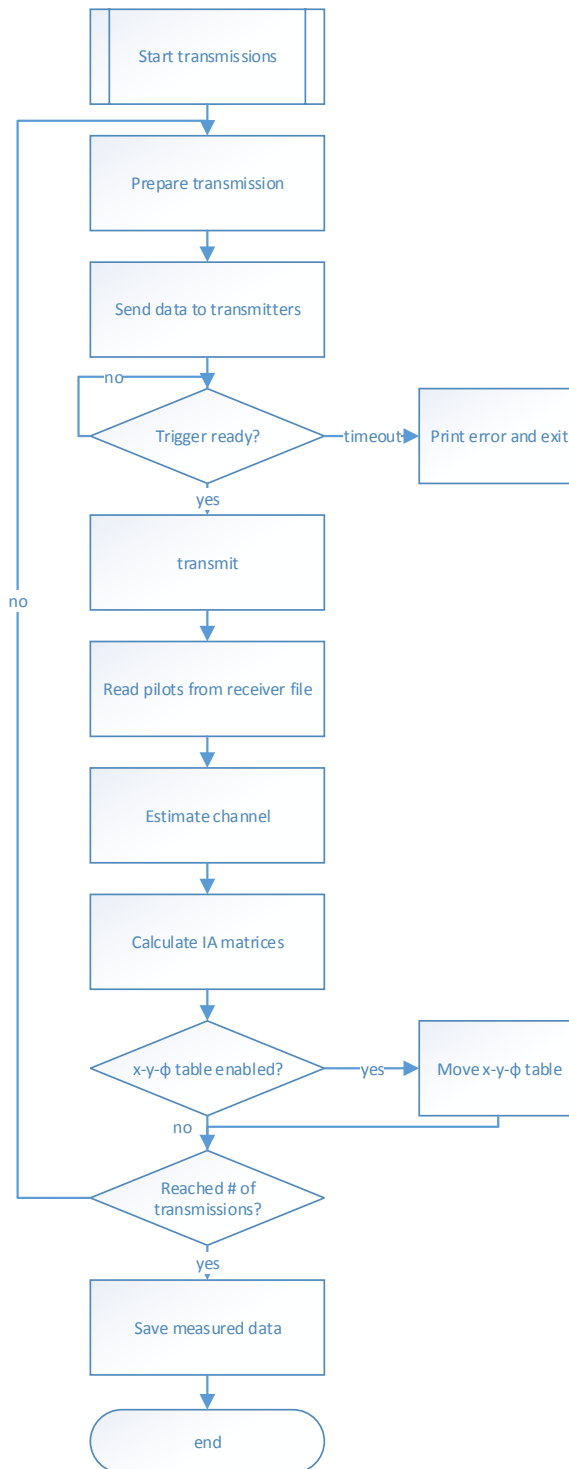**Figure 3.9.:** Initialization in the Matlab measurement script at the receiver

Figure 3.10.: Program flow of the measurement script while transmitting

Chapter 4.

Measurements and Results

4.1. Assumption Checks

Limits for several characteristic numbers are assumed in this thesis. Some of them are necessary in order for IA to work properly, others are taken to mask out already analyzed effects that should not influence the desired measurements.

It has been shown that IA outperforms other schemes in the high SNR regime [4]. In this work it is assumed that the SNR at the receiver is high enough so that IA is feasible.

In this thesis the dependency of IA performance on the movement of the receiver is investigated. It is supposed that the movement of the receiver causes the channels between the transmitters and the receiver to change and that the change of the channels between their estimation and the actual transmission of the precoded signals causes a decline in IA performance. Radio frequency channels change over time without receiver movement. In order to measure the dependency of IA performance on the movement, it has to be ensured that the channel changes over time are negligible when compared to channel changes due to receiver movement.

It is assumed that all transmit signals are received with the same power on average. This makes sense because if the transmit power of the desired transmitter is large compared to the other transmitters, then the interference on the receiver is low. In such a case the application of an interference channel model is unnecessary and IA is outperformed by other transmission schemes.

In a telecommunication system with mobile users the synchronization between the receivers and the base stations is imperfect. It is assumed that the nodes are synchronized well enough to mitigate these effects.

4.1.1. Delays

The time between consecutive transmissions should be short for several reasons. **U** and **V** are based on channel estimates from the previous transmissions (see Section 2.4.3). If the channel changes between transmissions then the IA precoders and filters might be outdated and interference won't be aligned properly. In order to keep the channels as constant as possible the time between two consecutive transmissions should be as short as possible.

The real-time testbeds presented in Section 1.1 can be used as benchmarks for the achievable delays in IA measurements. The installation in [4] has a delay of five seconds between a training phase during which the pilots are transmitted and the transmission of precoded data. In [6] it was claimed that the time between the transmission of the pilots and the precoded data was around *"a tenth of a second"*.

The implementation of schemes utilizing CSI feedback introduces additional delays. The received pilot samples need to be decoded at the receivers and the channels need to be estimated and fed back to the transmitters. Note that due to the assumption of perfect CSI distribution (see Section 3.2) those delays will not be investigated here.

On the VMTB the average delay between the start of two consecutive transmissions was evaluated to be $17ms$, with a standard deviation of $538\mu s$. It was found that writing files on hard disk drives (HDDs) takes a significant amount of time, so does reading from HDDs. This time was significantly reduced by using RAMdisk and increasing the personal computers random access memory (RAM) at Rx. Typical values for these delays can be found in Table 4.1

IA matrices are calculated with the analytical solution for the $(4 \times 4, 2)^3$ case (see [12]). The calculation of these IA matrices is fast compared to other tasks.

Table 4.2 compares delays for different numbers of transmit symbols. Time required for reading and writing from/to RAMdisks/HDDs, sending data to the transmitters over the network and transmitting over the physical channel scale with the number of transmit symbols. The length of the transmit signal is constant if cyclic prefix, pilot sequence and the number of data symbols are constant.

Measurements have shown that outdated CSI due to the achieved latencies is small enough to not influence the measurements conducted in Sections 4.3 and 4.3 significantly.

	μ	σ
calculate V, U	$514\mu s$	$144\mu s$
channel estimation	$3ms$	$38.4\mu s$
read pilot samples from RAMdisk	$2.4ms$	$39\mu s$
overall delay with RAMdisk	$17ms$	$538\mu s$
overall delay with HDD	$28ms$	$10ms$

Table 4.1.: Mean and standard deviation of feedback delays for IA measurements on the VMTB, $N_M = 200$, 10 data symbols per transmission

# of data symbols	10	20	50	100
overall delay μ	$17ms$	$23ms$	$50ms$	$107ms$
overall delay σ	$538\mu s$	$518\mu s$	$1.4ms$	$3.4ms$

Table 4.2.: Overall delays for different number of transmit symbols, $N_M = 200$ per column

4.1.2. Static Channels

Because the IA matrices which are calculated from frame l are applied at frame $l + 1$, changes of the wireless channel significantly reduce the performance of IA and schemes that exploit CSI in general. Channel changes are often caused by moving objects such as cars, pedestrians or trees that move in the wind. Because this work investigates the sensitivity of IA to receiver movement, it has to be assumed that channels only change due to location changes and are static otherwise. In practice this means that one must ensure that the changes of the channel and the impairments of the performance are caused mainly by the moving receiver and not by other effects. The VMTB was set up for all measurements in this thesis such that no streets lie between the transmitters and the receiver (see Figure 3.1). There are however some trees in the link. To mitigate the effects of moving trees, all measurements were performed on sunny, rainless, wind still days with a wind speed < 5km/h measured at the weather station at Tx2. Additionally there were no people or moving objects present inside the laboratory where Rx is located while measurements were performed.

To compare unwanted impairments to the performance due to a moving receiver, measurements where the receiver stood still were performed. The IA solution is calculated only from the channel estimates of first transmission $\widehat{\mathbf{H}}^{(1)}$ and is left constant during a measurement, this allows a measurement of the impact of outdated CSI on the MI. The receiver changes position and orientation between measurements but stands still during a measurement, $N_M = 50$ measurements were performed. Figure 4.1 shows a measurement block of the MI from all transmitters with 95% confidence intervals.

The measurements presented in this section differ from Figure 4.8 in the used IA solution. Figures 4.1 and 4.2 use the solution of the first transmissions whereas in Figure 4.8 a new IA solution is calculated and applied after each transmission.
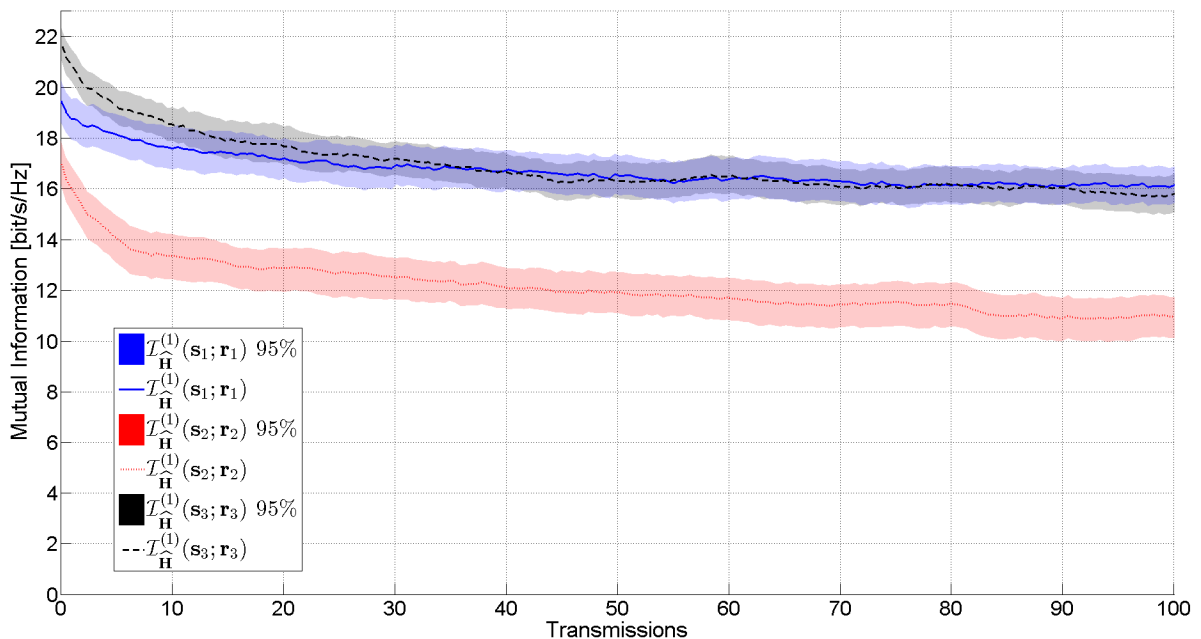

Figure 4.1.: MI with channel changing over time, averaged over $N_M = 50$ measurements with 95% confidence intervals of the mean
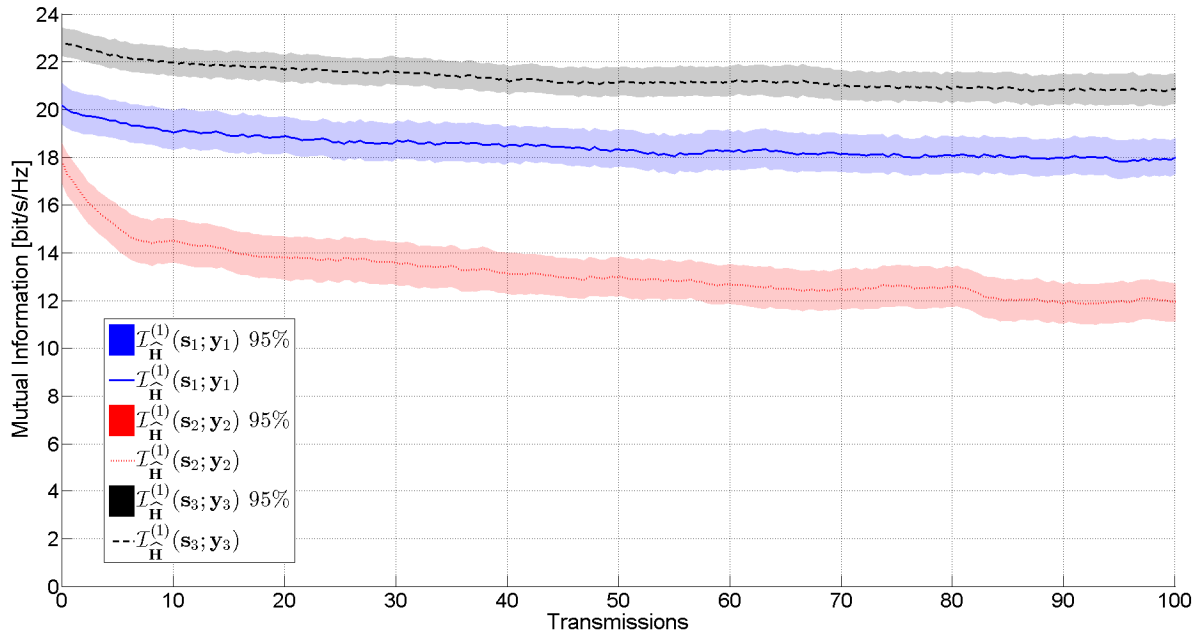
Figure 4.2.: MI with channel changing over time, no receive filters applied, averaged over $N_M = 50$ measurements with 95% confidence intervals of the mean

The x-axis can't be labeled as time because the time between transmissions is not equidistant, the average time for 100 transmissions was 1.7 seconds. Figure 4.1 shows the MI estimated from the channel matrices between **s** and **r** which means that the impact of both outdated transmit filters and outdated receive filters is shown, Figure 4.2 shows the same measurement block without applied receive filters. It can be seen that the MI declines by around 5bit/s/Hz without any receiver movement, which is significantly less than the results shown in Section 4.3.1 and Section 4.3.2.

4.1.3. Desired Transmitter turned off

If the desired transmitter is turned off the MI of the desired link should be zero. In measurements zero won't be achieved due to numerical errors and estimation errors resulting from the relatively small number of received symbols. Note that due to these errors the measured MI can be below zero. Significant deviations of the MI from zero in such a measurement might hint at a wrong implementation on the testbed.

Figure 4.3 shows a measurement block consisting of 50 measurements, where the desired transmitters were turned off. The receiver stood still during a measurement but moved to a random position and orientation between measurements. The resulting MI is close enough to zero for practical measurements.
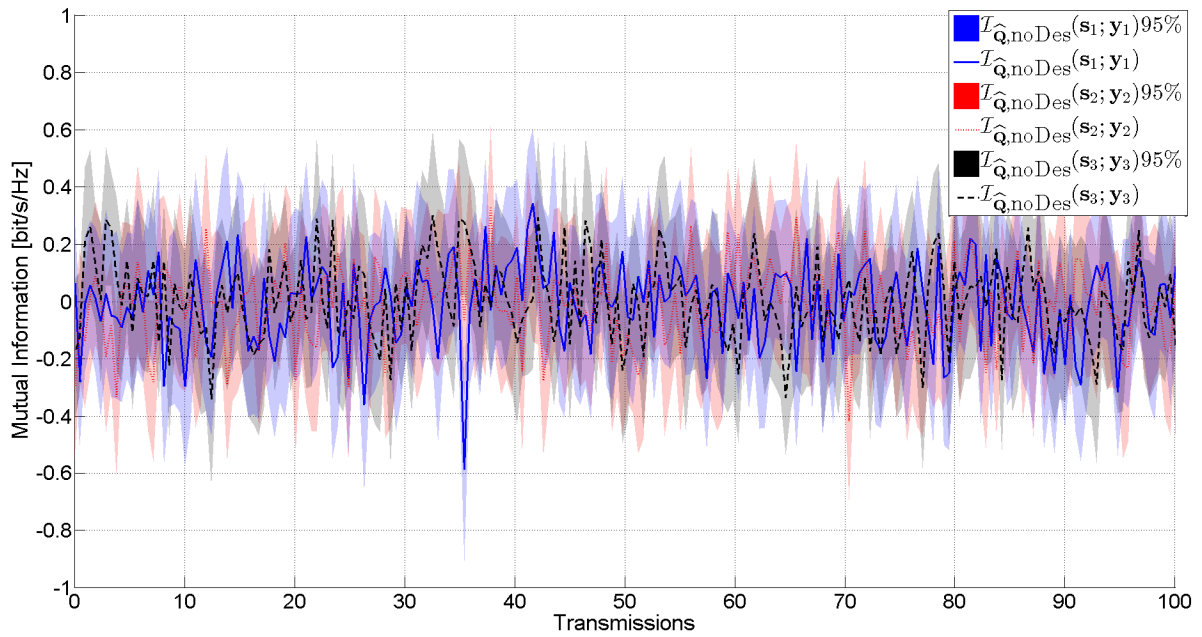
Figure 4.3.: Measurement of the MI where the desired transmitters were turned off, averaged over $N_M = 50$ measurements with 95% confidence intervals of the mean

4.1.4. Average equal received Power

IA was designed for scenarios with large interference, e.g. at cell edges of mobile communication systems. If no or only weak interference is present, IA is clearly outperformed by other schemes. In this work it is assumed that the desired and interfering signals are received with average equal power at the receiver, this results in a SIR of -3dB. The performance of IA under changing SIR is discussed in [9]. Because IA works best in the high SNR regime, the SNR at the receiver is chosen as high as possible. [22, 41 ff.] shows various saturation effects of the VMTB receiver. [9] shows that these effects start to occur over 40dB SNR. It also found the necessary attenuation settings at the transmitters to achieve 37dB and equal received power from all transmitters on average. Measurements with slightly less than 40dB SNR are therefore enough to outperform competing schemes like TDMA and Interference Avoidance[3] and low enough to avoid saturation effects at the receiver.

The received power from each transmitter is not constant at the receiver due to the receiver's movement. The attenuators at the transmitters are adjusted such that the power of all received signals is equal on average. Note that average is taken over table positions, different angles of the receive antennas and time. This implies that the received power averages resulting from the different transmitters will in general not have to be same during a single measurement. Figure 4.4 shows a typical measurement of the received signal powers. In this measurement the receiver stands still for ten transmissions and moves in a given direction between these blocks. It is evident that the received power varies between different receiver positions but is within the same magnitude.
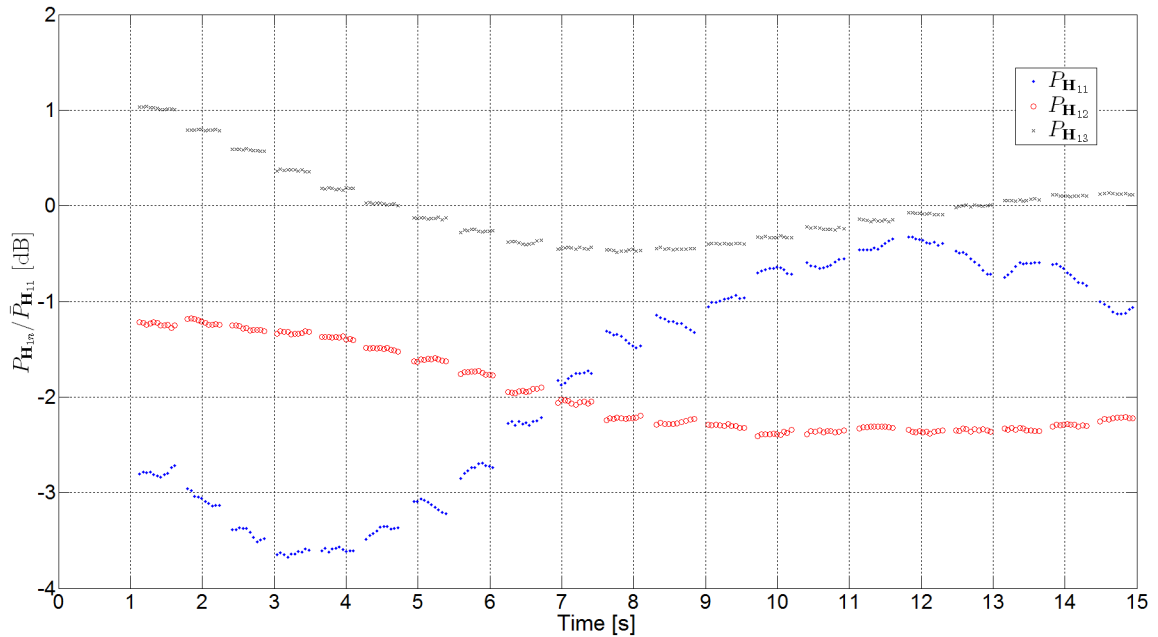

Figure 4.4.: Typical measurement of the received power from each transmitter over time, normalized to the average received power from Tx1

4.2. IA in a static Scenario

All measurements in this chapter are preformed with 37dB SNR and -3dB SIR. The receiver does not move during a measurement, new IA solutions are calculated and applied between consecutive transmissions. These assumptions do not mean that the measurements in this chapter resemble the performance of IA in a commercial system. The differences to commercial systems originating from the used measurement setup that were discussed in Section 3.2 are still in effect.

Figure 4.5 shows a measurement block consisting of 50 measurements where Tx1 was the desired transmitter. It can be seen that if no interferers are present SVD outperforms IA ("half the cake"). If interferers are present, SVD performs poorly and is outperformed by IA. Here SVD performs especially bad because all transmitters are received with approximately the same power. In this testbed environment IA with interferers performs almost as well as the emulated case without interferers. Figures 4.6 and 4.7 show measurement blocks with the same settings for desired transmitters Tx2 and Tx3. Figure 4.8 compares the measured MI of the various transmitters under perfect IA conditions.
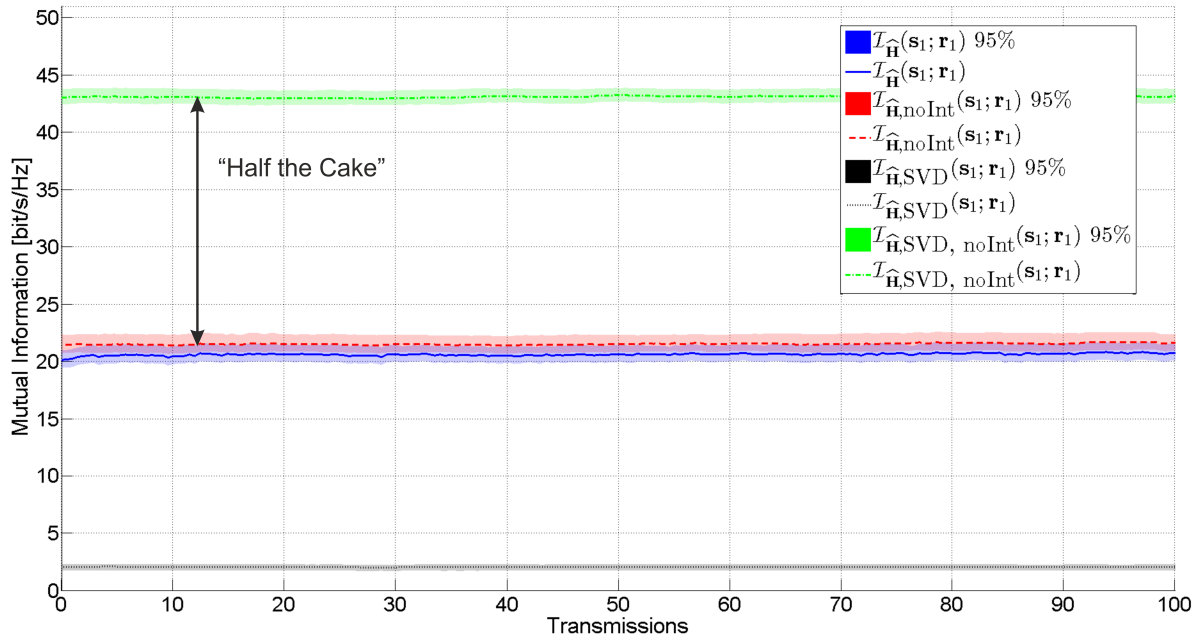
Figure 4.5.: IA, link 1, compared to SVD and IA without interferers, averaged over $N_M = 50$ measurements with 95% confidence intervals of the mean
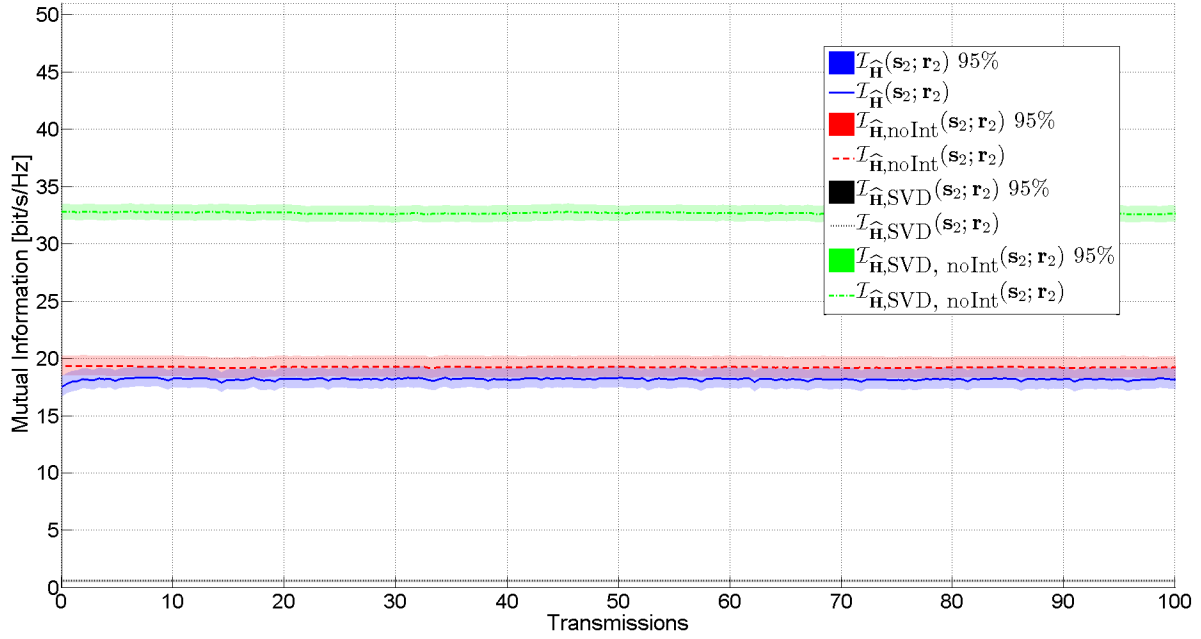
Figure 4.6.: IA, link 2, compared to SVD and IA without interferers, averaged over $N_M = 50$ measurements with 95% confidence intervals of the mean
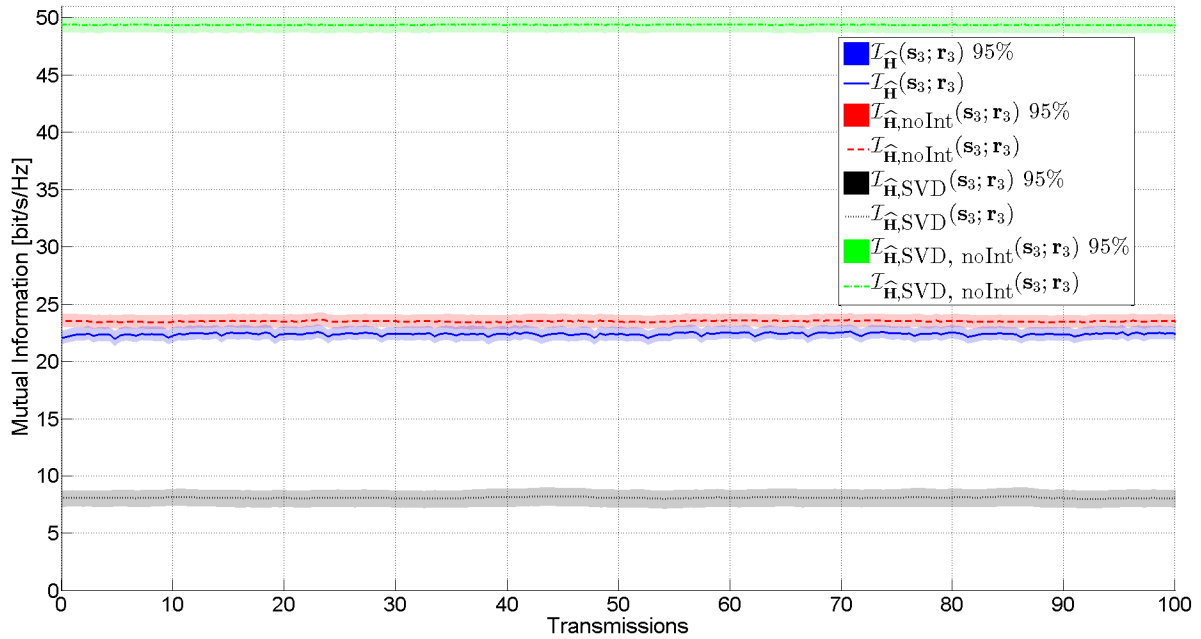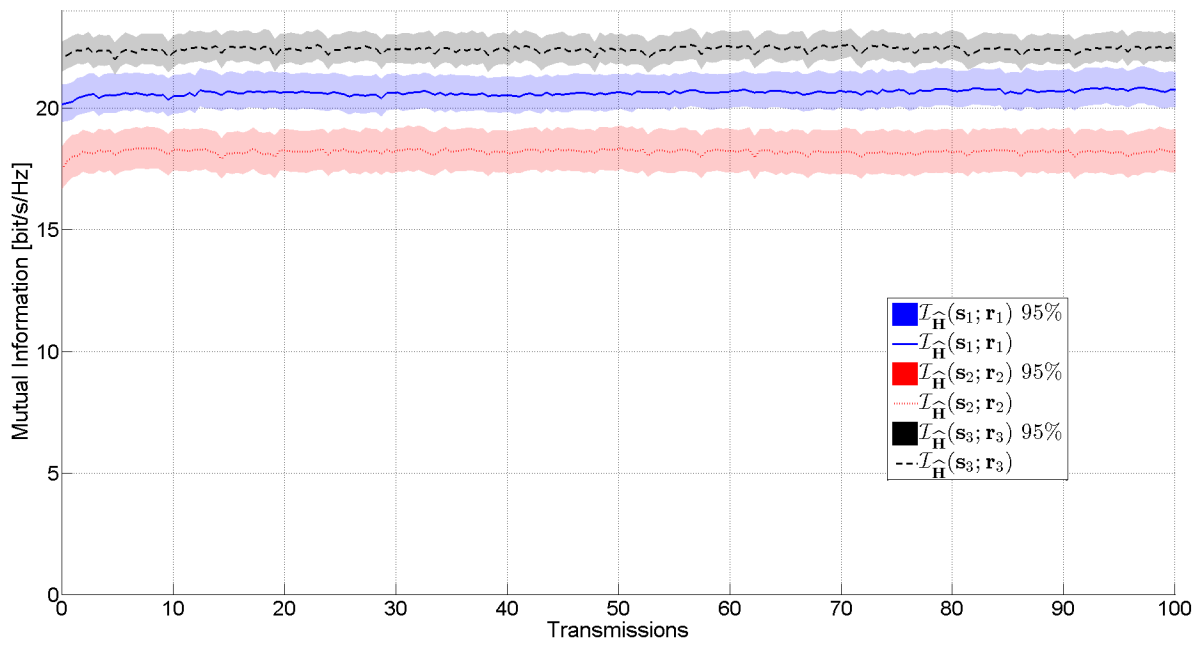

Figure 4.7.: IA, link 3, compared to SVD and IA without interferers, averaged over $N_M = 50$ measurements with 95% confidence intervals of the mean

Figure 4.8.: IA, comparison between desired transmitters, averaged over $N_M = 50$ measurements with 95% confidence intervals of the mean

4.3. IA under Receiver Movement

In this chapter the influence of receiver location changes on the performance of IA is investigated. The receiver stood still during transmissions which means that these measurements do not contain effects of Doppler shift and are therefore only valid for small speeds. The transmitters stood still during all times which is a usual assumption in current mobile communication systems as both cellular base stations and WLAN routers are stationary. Measurements in this chapter show that IA is outperformed by SVD after the receiver moved some tenths of wavelength. Additionally the quantitative results in this chapter provide a well-grounded basis for pilot design in IA and allow an approximation of IA performance for existing pilot designs.

4.3.1. One Wavelength

In this section blocks of measurements are presented where the receiver moves 0.1 wavelengths into until it is 1.2 wavelengths away from the initial position. Between measurements the receiver moves to a random position and aligns the laptop chassis in a random direction between -45° and 45°. The movement direction, starting position and angle of the receive antennas are randomly changed between measurements. At each position the receiver stands still and 10 frames are transmitted before moving to the next position. 100 measurements were performed during each measurement block resulting in $N_M = 1000$ realizations for each point. The IA solution of the first transmission is kept for an entire measurement.

Figure 4.9, Figure 4.10 and Figure 4.11 show the performance of IA as a function of receiver location over one wavelength. Figure 4.12 compares the results from Figures 4.9 to 4.11. Figure 4.13 shows the performance without receive filters.
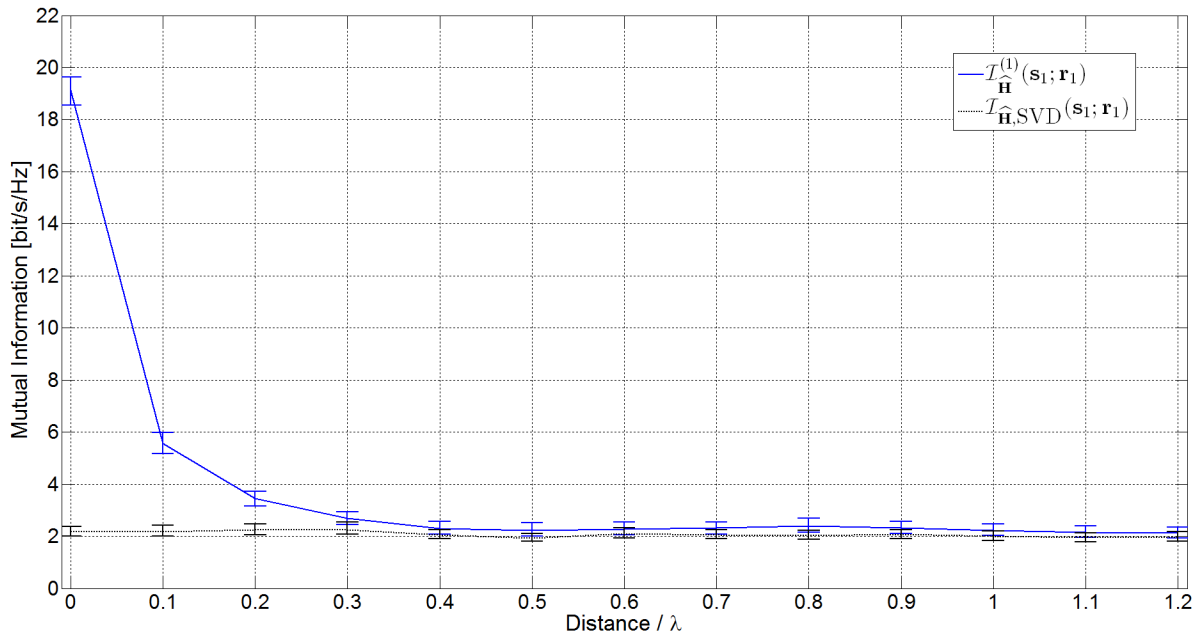

Figure 4.9.: MI of IA as a function of receiver movement, desired transmitter 1, averaged over $N_M = 1000$ measurements with 95% confidence intervals of the mean
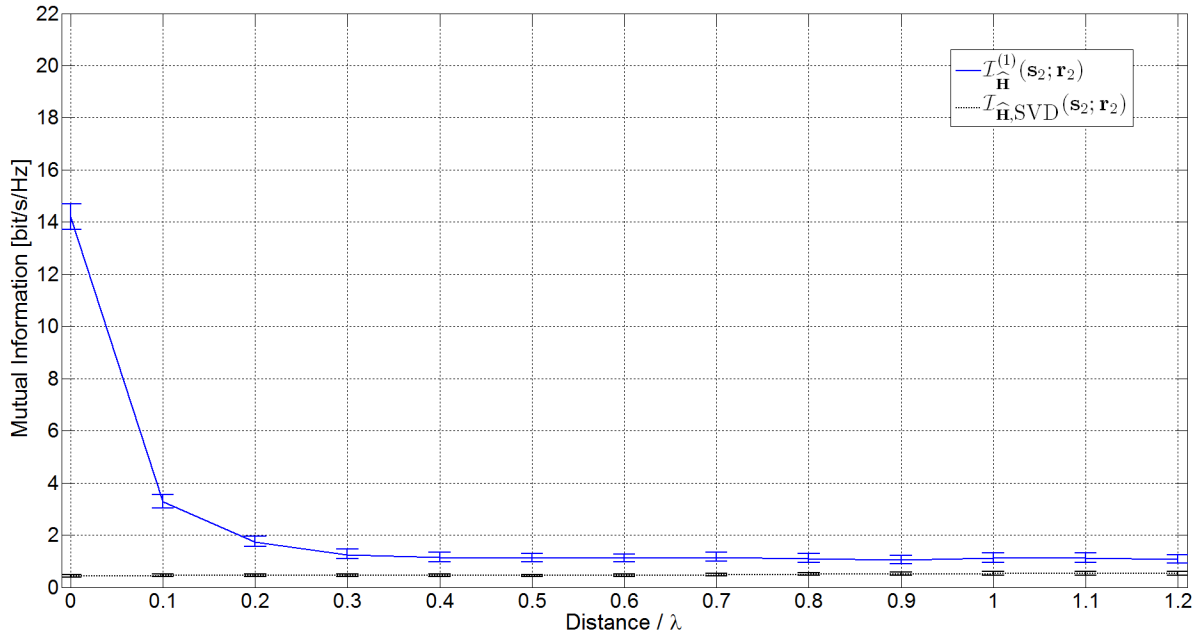
Figure 4.10.: MI of IA as a function of receiver movement, desired transmitter 2, averaged over $N_M = 1000$ measurements with 95% confidence intervals of the mean
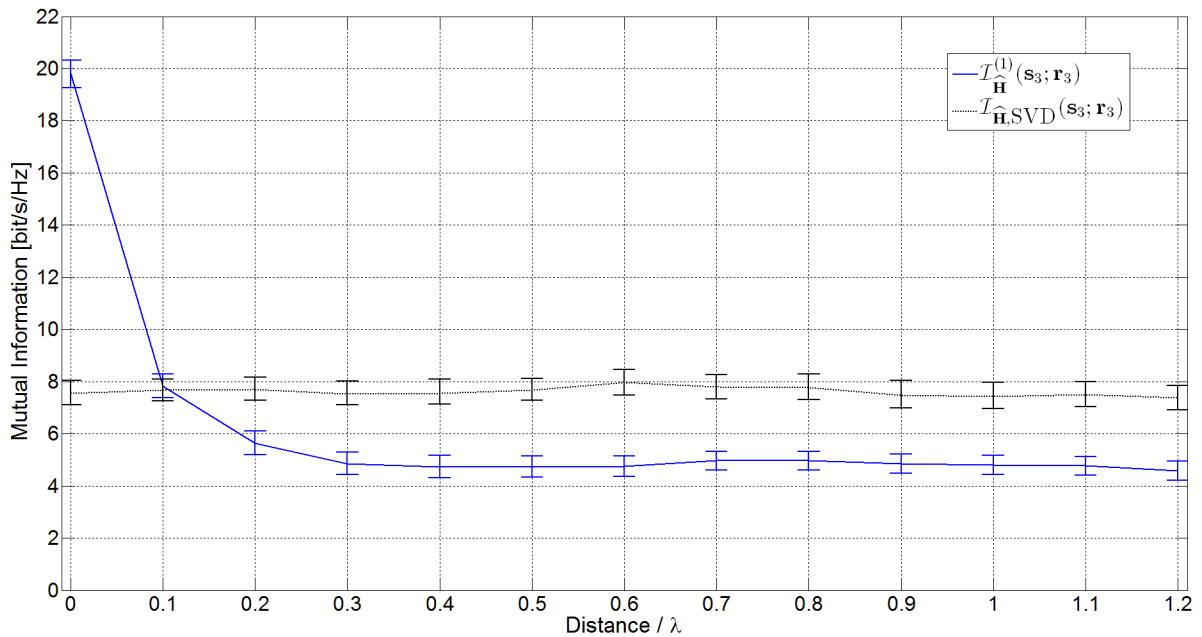

Figure 4.11.: MI of IA as a function of receiver movement, desired transmitter 3, averaged over $N_M = 1000$ measurements with 95% confidence intervals of the mean
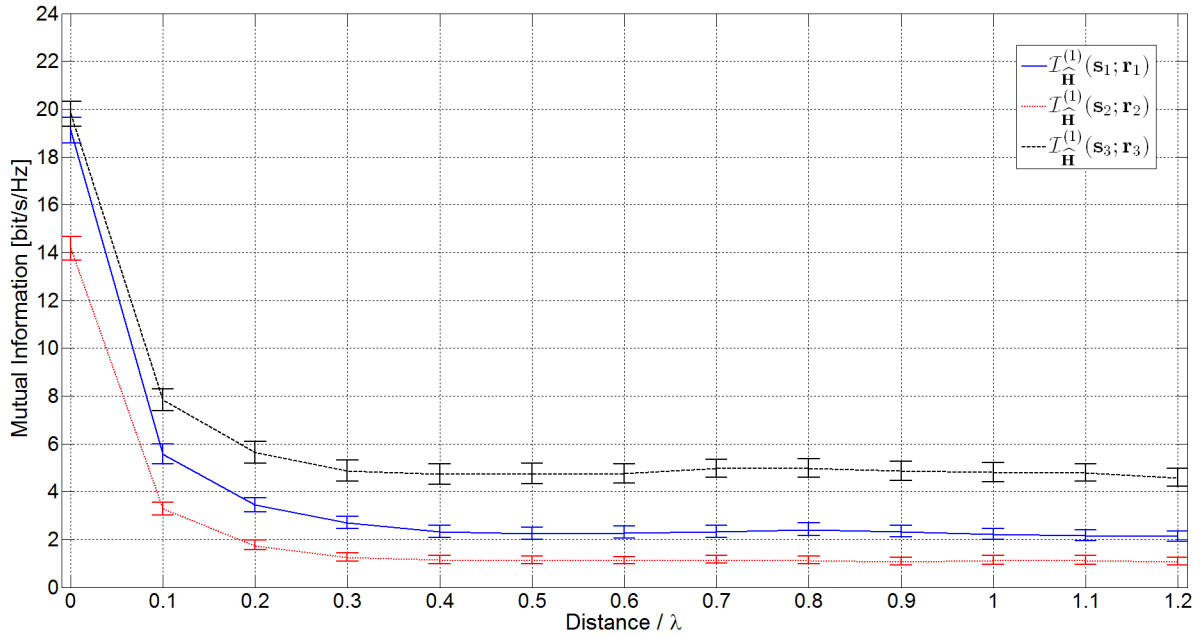
Figure 4.12.: MI of IA as a function of receiver movement, comparison, averaged over $N_M = 1000$ measurements with 95% confidence intervals of the mean
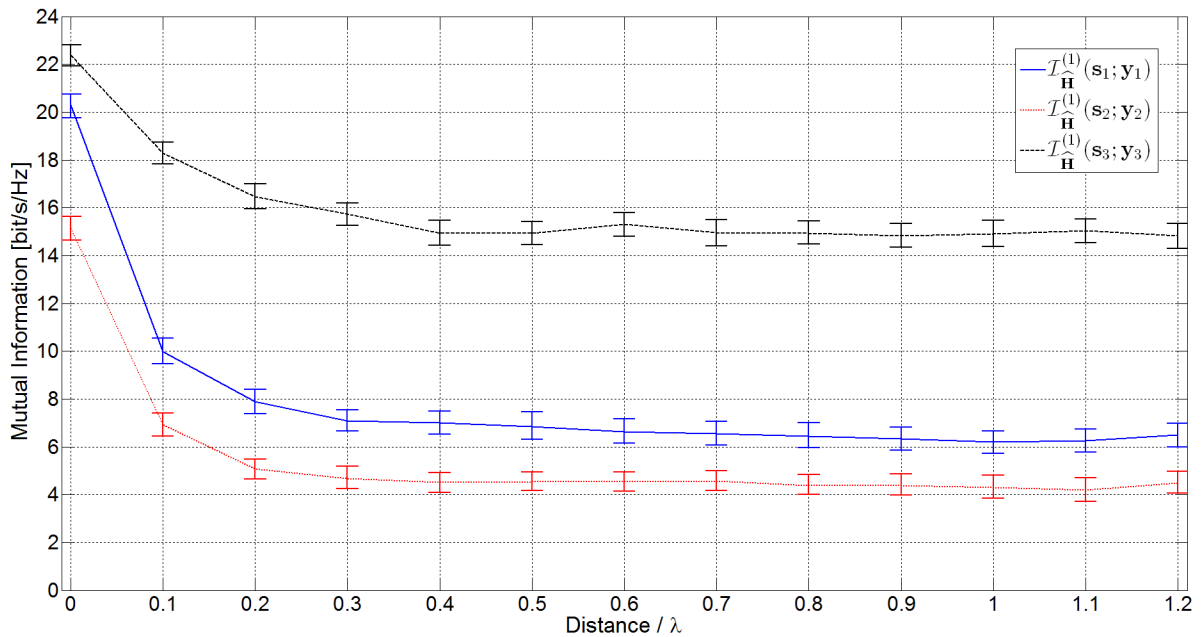

Figure 4.13.: MI of IA as a function of receiver movement, no receive filters, comparison, averaged over $N_M = 1000$ measurements with 95% confidence intervals of the mean

4.3.2. Half Wavelength

Measurements in Section 4.3.1 show that the MI decreases quite rapidly with traveled distance. For design purposes only low decreases in performance are relevant. In-depth measurements were performed to provide more detailed results over half a wavelength.

Figures 4.14 and 4.15 show measurements similar to those conducted in Section 4.3.1 but measured in more steps over half a wavelength of receiver movement.
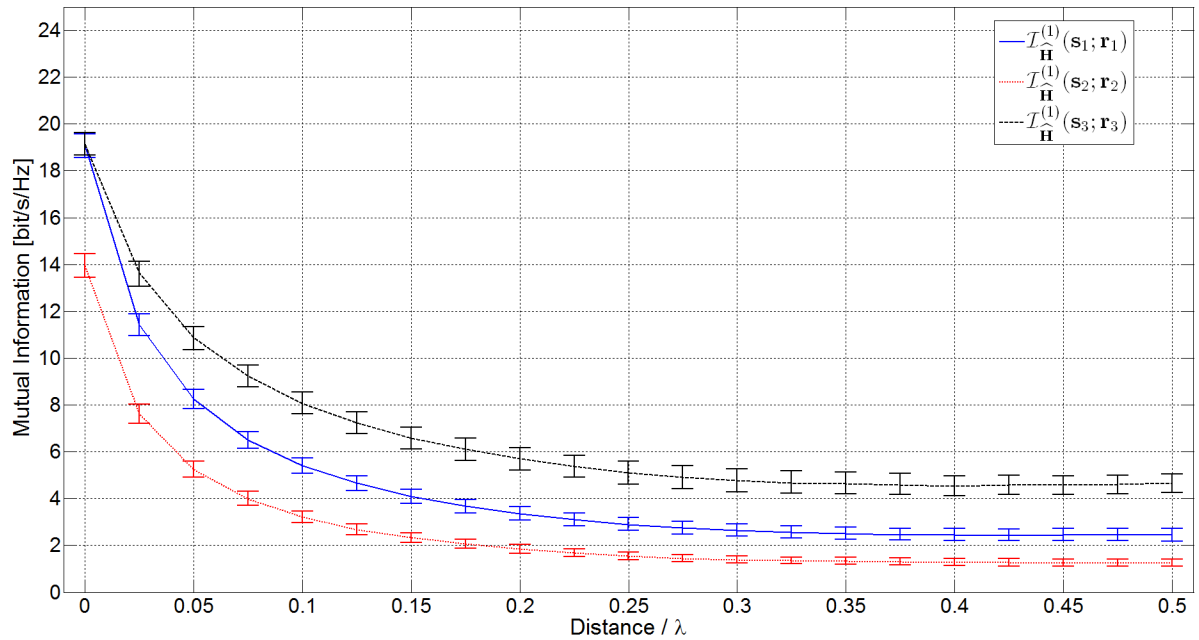

Figure 4.14.: MI of IA as a function of receiver movement over half a wavelength, averaged over $N_M = 1000$ measurements with 95% confidence intervals of the mean
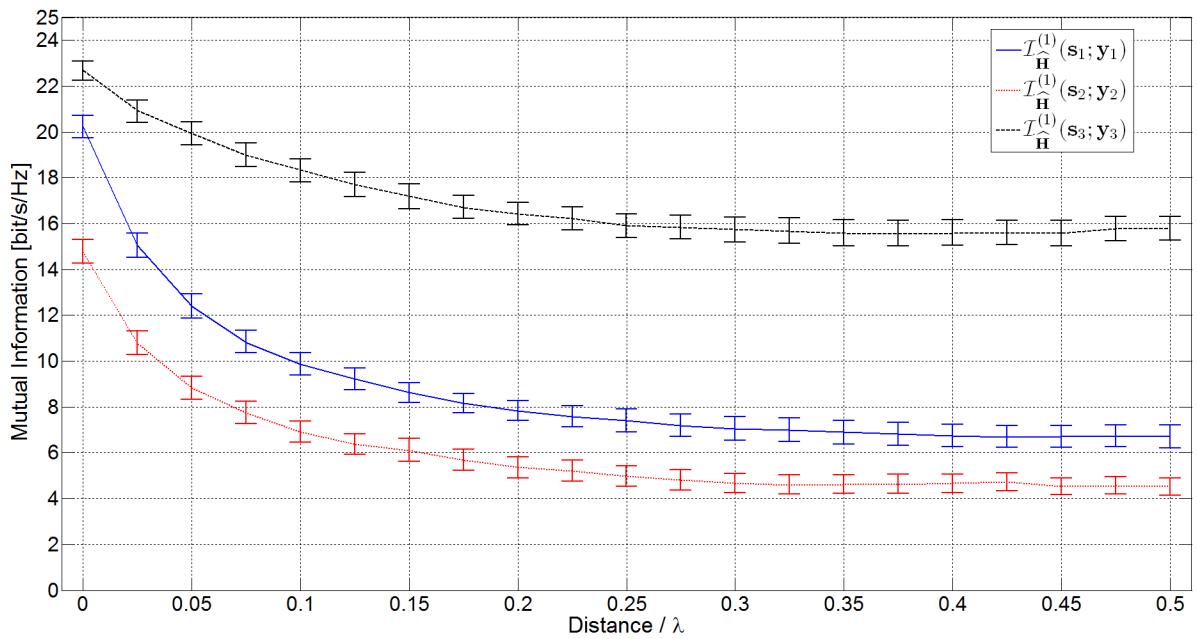
Figure 4.15.: MI of IA as a function of receiver movement over half a wavelength, no receive filters, averaged over $N_M = 1000$ measurements with 95% confidence intervals of the mean

Chapter 5.

Conclusion and Outlook

For the use of IA in future mobile communication standards and the appliance in commercial mobile communication systems thoroughly measurement based evaluations are necessary. In this thesis IA was implemented on the Vienna MIMO testbed (VMTB) and a measurement based evaluation in an in- and outdoor scenario was presented. Measurements of the performance of IA in static scenarios and with a moving receiver have been conducted as part of this thesis.

Measured quantitative results on the performance of IA in a static scenario presented in Section 4.1.2 have shown that the performance degrades slowly over time. This finding emphasizes the application of IA in communication systems with slowly changing channels and little receiver movement (e.g. laptops in WLAN).

For moving receivers CSI needs to be fed back more often to prevent outdated precoders. However a higher pilot denseness reduces the performance as it occupies space of data symbols. I have presented a measurement method to quantify the performance of feedback schemes (e.g. IA) under receiver movement.

Measurements of the performance of IA where the receiver is moving provide a basis to design pilot patterns for channel estimation. As pilot symbols occupy the space of data symbols, scientific investigation of optimal pilot patterns is emphasized in order to utilize base station cooperative schemes in future mobile communication standards. There is ongoing research on feedback quantization [26] [27] [28] [29], delayed CSI at the transmitters [30] [31], IA techniques that don't require channel knowledge at the transmitters [32] [33] [34] and prediction models that extrapolate CSI [35] [36]. However, to the best of my knowledge these techniques have not been investigated in a real-time environment yet.

Although the VMTB was not designed for real time feedback and online signal generation, it has been shown that the VMTB is capable of performing these kinds of measurements. This knowledge has already spawned efforts to investigate pilot patterns and feedback in LTE on the VMTB. A high speed rotation unit was recently completed for the VMTB and it might be used to expand the work of this thesis to speeds up to 560 km/h.

List of Figures

Bibliography

[1] Shyamnath Gollakota, Samuel David Perli, and Dina Katabi. Interference alignment and cancellation. In *ACM SIGCOMM Computer Communication Review*, volume 39, pages 159–170. ACM, 2009.

[2] Omar El Ayach, Steven W Peters, and RW Heath. Real world feasibility of interference alignment using MIMO-OFDM channel measurements. In *Military Communications Conference, 2009. MILCOM 2009. IEEE*, pages 1–6. IEEE, 2009.

[3] Omar El Ayach, Steven W Peters, and Robert W Heath. The feasibility of interference alignment over measured MIMO-OFDM channels. *Vehicular Technology, IEEE Transactions on*, 59(9):4309–4321, 2010.

[4] O. González, D. Ramírez, I. Santamaria, J.A. García-Naya, and L. Castedo. Experimental validation of interference alignment techniques using a multiuser MIMO testbed. In *Smart Antennas (WSA), 2011 International ITG Workshop on*, pages 1–8, 2011.

[5] JA García-Naya, L Castedo, O González, D Ramírez, and I Santamaria. Experimental evaluation of interference alignemnt under imperfect channel state information. In *Proceedings of 19th European Signal Processing Conference (EUSIPCO)*. EUSIPCO, 2011.

[6] Per Zetterberg and Nima N Moghadam. An experimental investigation of SIMO, MIMO, interference-alignment (IA) and coordinated multi-point (CoMP). In *Systems, Signals and Image Processing (IWSSIP), 2012 19th International Conference on*, pages 211–216. IEEE, 2012.

[7] Rasmus Brandt, Henrik Asplund, and Mats Bengtsson. Interference alignment in frequency - a measurement based performance analysis. In *Systems, Signals and Image Processing (IWSSIP), 2012 19th International Conference on*, pages 227–230. IEEE, 2012.

[8] José A. Garcıa-Naya Cristian Lameiro, Óscar González and Luis Castedo. Experimental evaluation of interference alignment for broadband WLAN systems. unpublished, submitted to IEEE Transactions on Wireless Communications, arXiv:1309.4355 [cs.IT].

[9] Martin Mayer. Measurement based evaluation of interference alignment on the vienna MIMO testbed. Master's thesis, Technische Universität Wien, October 2013.

[10] M. Mayer, G. Artner, G. Hannak, M. Guillaud, and M. Lerch. Measurement based evaluation of interference alignment on the vienna MIMO testbed. In *The Tenth International Symposium on Wireless Communication Systems, (ISWCS 2013)*, Ilmenau, Germany, August 2013.

[11] J. Reitterer and M. Rupp. Interference alignment in umts long term evolution. In *Proc. European Signal Processing Conference 2011*, pages 1094–1098, Spain, August 2011.

[12] Viveck R .Cadambe and Syed A. Jafar. Interference alignment and degrees of freedom of the k-user interference channel. *IEEE transactions on information theory*, 54(8):3425–3441, 2008.

[13] Cenk M Yetis, Tiangao Gou, Syed A Jafar, and Ahmet H Kayran. On feasibility of interference alignment in MIMO interference networks. *Signal Processing, IEEE Transactions on*, 58(9):4771–4782, 2010.

[14] Krishna Gomadam, Viveck R Cadambe, and Syed A Jafar. Approaching the capacity of wireless networks through distributed interference alignment. In *Global Telecommunications Conference, 2008. IEEE GLOBECOM 2008. IEEE*, pages 1–6. IEEE, 2008.

[15] Jørgen Bach Andersen. Array gain and capacity for known random channels with multiple element arrays at both ends. *Selected Areas in Communications, IEEE Journal on*, 18(11):2172–2178, 2000.

[16] Jaiganesh Balakrishnan, Markus Rupp, and Harish Viswanathan. Optimal channel training for multiple antenna systems. *Multiaccess, mobility and teletraffic for wireless communications*, 5:25, 2000.

[17] Leonhard Edlinger. Vienna wireless testbed. Master's thesis, Technische Universität Wien, November 2011.

[18] Edin Huremović. Wireless testbed transmitter. Master's thesis, Technische Universität Wien, August 2011.

[19] M. Lerch and M. Rupp. Measurement-based evaluation of the LTE MIMO downlink at different antenna configurations. In *Proc. of 17th International ITG Workshop on Smart Antennas (WSA 2013)*, Stuttgart, Germany, March 2013.

[20] C. Mehlführer, S. Geirhofer, S. Caban, and M. Rupp. A flexible MIMO testbed with remote access. In *13. European Signal Processing Conference*, Antalya, Turkey, September 2005.

[21] S. Caban, C. Mehlführer, R. Langwieser, A.L. Scholtz, and M. Rupp. Vienna MIMO testbed. *EURASIP Journal on Applied Signal Processing*, Vol. 2006, Article ID 54868:1–13, 2006.

[22] Heinz Haderer. Wireless testbed receiver. Master's thesis, Technische Universität Wien, December 2011.

[23] Kathrein Inc., Scala Division. *800 10543, 800 10553, 60°XX-pol Panel Antenna 2300-2690 MHz.* http://antennasystems.com/Merchant2/pdf/800_10543.pdf, 26.4.2013.

[24] Kathrein Inc., Scala Division. *800 10677, Dualband Directional Indoor Antenna with Integrated Combiner.* http://www.kathrein-scala.com/catalog/80010677.pdf, 26.4.2013.

[25] Armin Dißlbacher Fink. Hardware-based timing synchronization. Master's thesis, Technische Universität Wien, December 2010.

[26] Rajesh T Krishnamachari and Mahesh K Varanasi. Interference alignment under limited feedback for MIMO interference channels. In *Information Theory Proceedings (ISIT), 2010 IEEE International Symposium on*, pages 619–623. IEEE, 2010.

[27] Mohsen Rezaee and Maxime Guillaud. Interference alignment with quantized grassmannian feedback in the k-user constant MIMO interference channel. *arXiv preprint arXiv:1207.6902*, 2012.

[28] Roland Tresch and Maxime Guillaud. Cellular interference alignment with imperfect channel knowledge. In *Communications Workshops, 2009. ICC Workshops 2009. IEEE International Conference on*, pages 1–5. IEEE, 2009.

[29] H B olcskei and IJ Thukral. Interference alignment with limited feedback. In *Information Theory, 2009. ISIT 2009. IEEE International Symposium on*, pages 1759–1763. IEEE, 2009.

[30] Mohammad Ali Maddah-Ali and David Tse. On the degrees of freedom of miso broadcast channels with delayed feedback. *EECS Department, University of California, Berkeley, Tech. Rep. UCB/EECS-2010-122*, 2010.

[31] Hamed Maleki, Syed Ali Jafar, and Shlomo Shamai. Retrospective interference alignment over interference networks. *Selected Topics in Signal Processing, IEEE Journal of*, 6(3):228–240, 2012.

[32] S.A. Jafar. Exploiting channel correlations - simple interference alignment schemes with no CSIT. In *Global Telecommunications Conference (GLOBECOM 2010), 2010 IEEE*, pages 1–5, 2010.

[33] Yan Zhu and Dongning Guo. The degrees of freedom of isotropic mimo interference channels without state information at the transmitters. *Information Theory, IEEE Transactions on*, 58(1):341–352, 2012.

[34] Tiangao Gou, Chenwei Wang, and S.A. Jafar. Aiming perfectly in the dark-blind interference alignment through staggered antenna switching. *Signal Processing, IEEE Transactions on*, 59(6):2734–2744, 2011.

[35] Nan Zhao, F.R. Yu, Hongjian Sun, Hongxi Yin, and A. Nallanathan. Interference alignment based on channel prediction with delayed channel state information. In *Global Communications Conference (GLOBECOM), 2012 IEEE*, pages 4244–4248, 2012.

[36] Heejung Yu, Youngchul Sung, Haksoo Kim, and Yong H. Lee. Beam tracking for interference alignment in slowly fading MIMO interference channels: A perturbations approach under a linear framework. *Signal Processing, IEEE Transactions on*, 60(4):1910–1926, 2012.

Appendix A.

Abbreviations

ADC	analog to digital converter
ARP	address resolution protocol
BER	bit error rate
BPSK	binary phase shift keying
CoMP	coordinated multi-point
CPU	central processing unit
CSI	channel state information
DAC	digital to analog converter
DoF	degrees of freedom
DRAM	dynamic random access memory
FFT	fast fourier transform
GPS	global positioning system
HDD	hard disk drive
IA	interference alignment
ISM	industrial, scientific and medical
LAN	local area network
LS	least squares
LTE	UMTS long term evolution
MI	mutual information
MIMO	multiple input multiple output
MSE	mean squared error
OFDM	orthogonal frequency-division multiplexing
PC	personal computer
QAM	quadrature amplitude modulation
RAM	random access memory
SAW	surface acoustic wave
SIR	signal to interference ratio
SNR	signal to noise ratio
SVD	singular value decomposition
TDMA	time division multiple access
USRP	universal software radio peripheral
VMTB	Vienna MIMO testbed
WLAN	wireless LAN

Appendix B.

Parameters on the VMTB

The software written for the evaluation of IA on the VMTB allows changes to various settings to adjust measurements. To make a repetition of the measurements conducted in this thesis possible, Table B.1 contains a compilation of the used settings. Triples [., ., .] represent the settings at Tx1, Tx2 and Tx3.

used training sequence	$[1,\ 1,\ 1,\ 1,\ 1,\ j,\ -1,\ -j,\ 1,\ -1,\ 1,\ -1,\ 1,\ -j,\ -1,\ j]$
# transmit symbols	30
# of subcarriers	1
# of streams	2
# of Tx antennas	4
# of Rx antennas	4
# of transmitters	3
# of receivers	1
use RamDisk	true
use FOT[1]	false
randomize Tx data	true
sample delay	[710, 710, 630]
testbed attenuators	[36, 38, 42]
gain factors	[1, 1, 1]
FFT length	1023
cyclic prefix length	76
resample factor	13
scheme	QPSK
IA algorithm	analytic
DAC scaling	$2^{14.3}$ / # of total Tx antennas
zero padding begin	1000 + SampPerSymPassBand
zero padding middle	1000
zero padding end	1000

Table B.1.: Settings on the VMTB

[1] "use FOT" only makes sense when a single subcarrier is used. When it is set true, the pilots for channel estimation are split up into three subcarriers that are adjacent to the subcarrier used for data transmission. This allows a pilot length of one third the initial length and speeds up the transmission of the signal, but might introduce additional errors to the channel estimates.